AD-A077 024 ROME AIR DEVELOPMENT CENTER GRIFFISS AFB NY F/G 17/9
TROPOSPHERIC REFRACTIVE STUDIES FOR SPADATS RADAR SITES,(U)
MAY 79 L E TELFORD
UNCLASSIFIED RADC-TR-79-177 NL

1 OF 1
AD
A077024



END
DATE
FILMED
1-80
DDC

AD A077024

RADC-TR-79-177
In-House Report
May 1979

LEVEL II

TROPOSPHERIC REFRACTIVE STUDIES FOR SPADATS RADAR SITES

Larry E. Telford

DDC
RECEIVED
NOV 21 1979
E

APPROVED FOR PUBLIC RELEASE; DISTRIBUTION UNLIMITED

DDC FILE COPY

ROME AIR DEVELOPMENT CENTER
Air Force Systems Command
Griffiss Air Force Base, New York 13441

309 050
79 11 19 122

This report has been reviewed by the RADC Information Office (OI) and is releasable to the National Technical Information Service (NTIS). At NTIS it will be releasable to the general public, including foreign nations.

RADC-TR-79-177 has been reviewed and is approved for publication.

APPROVED: Edward A. Lewis

EDWARD A. LEWIS
Chief, Propagation Branch
Electromagnetic Sciences Division

APPROVED: Allan C. Schell

ALLAN C. SCHELL, Chief
Electromagnetic Sciences Division

FOR THE COMMANDER: John P. Huss

JOHN P. HUSS
Acting Chief, Plans Office

If your address has changed or if you wish to be removed from the RADC mailing list, or if the addressee is no longer employed by your organization, please notify RADC (EEP) Hanscom AFB MA 01731. This will assist us in maintaining a current mailing list.

Do not return this copy. Retain or destroy.

MISSION
of
Rome Air Development Center

RADC plans and executes research, development, test and selected acquisition programs in support of Command, Control Communications and Intelligence (C^3I) activities. Technical and engineering support within areas of technical competence is provided to ESD Program Offices (POs) and other ESD elements. The principal technical mission areas are communications, electromagnetic guidance and control, surveillance of ground and aerospace objects, intelligence data collection and handling, information system technology, ionospheric propagation, solid state sciences, microwave physics and electronic reliability, maintainability and compatibility.

Printed by
United States Air Force
Hanscom AFB, Mass. 01731

Unclassified

SECURITY CLASSIFICATION OF THIS PAGE (When Data Entered)

REPORT DOCUMENTATION PAGE		READ INSTRUCTIONS BEFORE COMPLETING FORM
1. REPORT NUMBER RADC-TR-79-177	2. GOVT ACCESSION NO.	3. RECIPIENT'S CATALOG NUMBER
4. TITLE (and Subtitle) TROPOSPHERIC REFRACTIVE STUDIES FOR SPADATS RADAR SITES		5. TYPE OF REPORT & PERIOD COVERED In-House Report 6. PERFORMING ORG. REPORT NUMBER
7. AUTHOR(s) Larry E. Telford		8. CONTRACT OR GRANT NUMBER(s)
9. PERFORMING ORGANIZATION NAME AND ADDRESS Deputy for Electronic Technology (RADC/EEP) Hanscom AFB Massachusetts 01731		10. PROGRAM ELEMENT, PROJECT, TASK AREA & WORK UNIT NUMBERS 62702F 46001602
11. CONTROLLING OFFICE NAME AND ADDRESS Deputy for Electronic Technology (RADC/EEP) Hanscom AFB Massachusetts 01731		12. REPORT DATE May 1979 13. NUMBER OF PAGES 70
14. MONITORING AGENCY NAME & ADDRESS(if different from Controlling Office)		15. SECURITY CLASS. (of this report) Unclassified 15a. DECLASSIFICATION/DOWNGRADING SCHEDULE

16. DISTRIBUTION STATEMENT (of this Report)

Approved for public release; distribution unlimited.

17. DISTRIBUTION STATEMENT (of the abstract entered in Block 20, if different from Report)

18. SUPPLEMENTARY NOTES

19. KEY WORDS (Continue on reverse side if necessary and identify by block number)

ADCOM
SPADATS
Tropospheric refraction correction
Tropospheric refractive bending
Tropospheric refractive range error

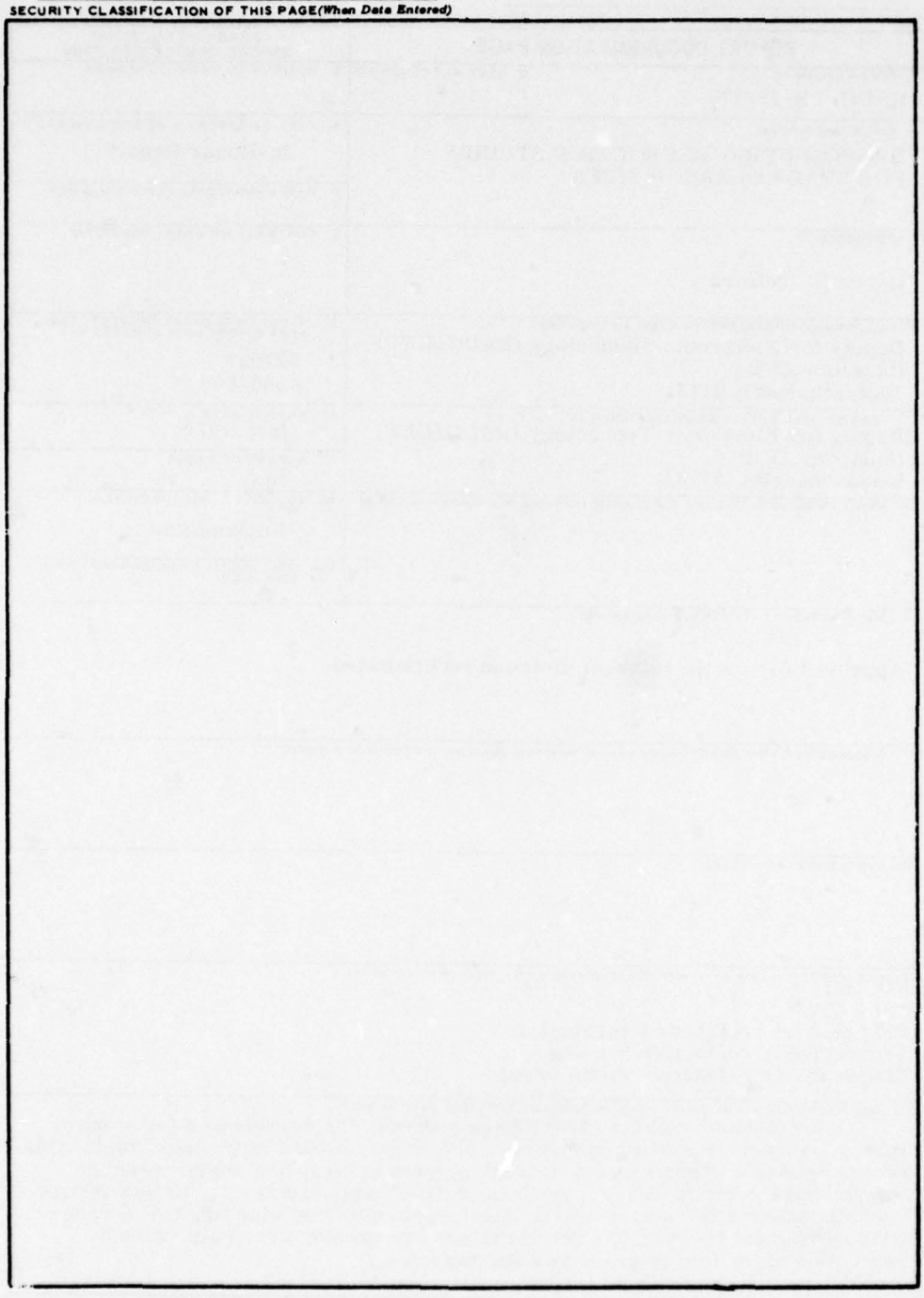
20. ABSTRACT (Continue on reverse side if necessary and identify by block number)

As prediction tracking radars have evolved, the corrections for tropospheric refractive bending and range error have become more important. Current operational requirements to track targets at elevation angles near the horizon have complicated tropospheric refraction corrections. In this report the tropospheric refractive environment is examined at nine SPADATS radar sites throughout the world. Site statistics are presented and a proposed correction algorithm is presented and tested.

DD FORM 1 JAN 73 1473 EDITION OF 1 NOV 65 IS OBSOLETE

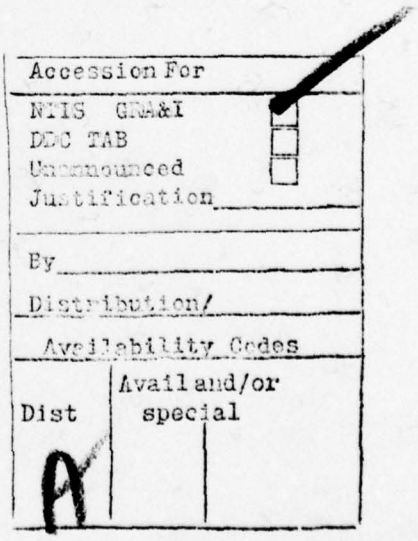
Unclassified

SECURITY CLASSIFICATION OF THIS PAGE (When Data Entered)



Preface

The author wishes to express his thanks to John Doherty who provided all the programming necessary to convert the USAFETAC raw data tapes to a useful format.



Contents

1.	INTRODUCTION	9
2.	APPROACH	12
3.	COMPUTATION OF DATA BASE	16
4.	NUMERICAL RESULTS (Site Statistics)	19
	4.1 Fylingdales, England	21
	4.2 Thule, Greenland	21
	4.3 Clear, Alaska	22
	4.4 Eglin AFB, Florida	24
	4.5 Diyarbakir, Turkey	25
	4.6 Shemya, Alaska	26
	4.7 Canton Island	26
	4.8 Ascension Island	27
	4.9 Guam	28
5.	CORRECTION METHODS AND RESULTS	45
	5.1 Fylingdales, England	52
	5.2 Thule, Greenland	52
	5.3 Clear, Alaska	52
	5.4 Eglin AFB, Florida	53
	5.5 Dyarbakir, Turkey	53
	5.6 Shemya, Alaska	53
	5.7 Canton Island	54
	5.8 Ascension Island	54
	5.9 Guam	54
6.	SUMMARY AND CONCLUSIONS	64
7.	RECOMMENDATIONS	64
REFERENCES		67
APPENDIX A:	Correction Algorithm Form	69

Illustrations

1.	Radar Path Geometry	11
2a.	Typical Range Error vs Elevation Angle	11
2b.	Typical Refractive Bending vs Elevation Angle	12
A1.	Schematic Representation of Ray Path	70

Tables

1.	Primary and Secondary Site Locations	15
2.	Elevation Angles Used in Refraction Analysis	19
3a.	Fylingdales Site Statistics	29
3b.	Fylingdales Site Difference Statistics	30
4a.	Thule Site Statistics	31
4b.	Thule Site Difference Statistics	32
5a.	Clear Site Statistics	33
5b.	Clear Site Difference Statistics	34
6a.	Eglin Site Statistics	35
6b.	Eglin Site Difference Statistics	36
7a.	Diyarbakir Site Statistics	37
7b.	Diyarbakir Site Difference Statistics	38
8a.	Shemya Site Statistics	39
8b.	Shemya Site Difference Statistics	40
9a.	Canton Island Site Statistics	41
9b.	Canton Island Site Difference Statistics	42
10.	Ascension Island Site Statistics	43
11.	Guam Site Statistics	44
12.	Surface Refractive Index Values	50
13a.	Site Coefficients for Range Algorithm	50
13b.	Site Coefficients for Refractive Bending Algorithm	51
13c.	Site Coefficients for Elevation Angle Algorithm	51
14a.	Fylingdales Range Error (m) Algorithm Test Results	55
14b.	Fylingdales Refractive Bending (deg) Algorithm Test Results	55
15a.	Thule Range Error (m) Algorithm Test Results	56
15b.	Thule Refractive Bending (deg) Algorithm Test Results	56
16a.	Clear Range Error (m) Algorithm Test Results	57

Tables

16b.	Clear Refractive Bending (deg) Algorithm Test Results	57
17a.	Eglin Range Error (m) Algorithm Test Results	58
17b.	Eglin Refractive Bending (deg) Algorithm Test Results	58
18a.	Diyarbakir Range Error (m) Algorithm Test Results	59
18b.	Diyarbakir Refractive Bending (deg) Algorithm Test Results	59
19a.	Shemya Range Error (m) Algorithm Test Results	60
19b.	Shemya Refractive Bending (deg) Algorithm Test Results	60
20a.	Canton Island Range Error (m) Algorithm Test Results	61
20b.	Canton Island Refractive Bending (deg) Algorithm Test Results	61
21a.	Ascension Island Range Error (m) Algorithm Test Results	62
21b.	Ascension Island Refractive Bending (deg) Algorithm Test Results	62
22a.	Guam Range Error (m) Algorithm Test Results	63
22b.	Guam Refractive Bending (deg) Algorithm Test Results	63

Tropospheric Refractive Studies for SPADATS Radar Sites

1. INTRODUCTION

This report is in response to a request by Headquarters, Electronic Systems Division (ESD) to investigate the tropospheric refractive environment for a number of U.S. Air Force Air Defense Command radars used for surveillance and tracking of artificial earth satellites. This investigation includes the development and testing of correction algorithms which predict tropospheric range error and angle bending.

The increasing number of space objects having nearly the same orbit has added to the difficulty of maintaining accurate, up-to-date orbital elements for each object. The SPADATS/SPACETRACK radars tasked with this mission have been given greater accuracy requirements which in turn require more precise trospheric and ionospheric refraction corrections as well as improvements in the radar systems. This report will consider the tropospheric refraction effects only; the ionospheric refraction effects on the SPADATS radars have been reported by Klobuchar and Allen. [1] All references to refractive effects in this report will be tropospheric only with no consideration of the effects of the ionosphere on the radar waves.

(Received for publication 4 June 1979)

1. Klobuchar, J.A., and Allen, R.S. (1976) Maximum Ionospheric Range Error For Air Defense Command Radars, AFGL-TR-76-0042, AD BO11322L.

The radar locations represent a wide range of climatological conditions ranging from tropical in the South Pacific to arctic in Greenland. The nine primary SPADATS radar locations analyzed in this report are as follows:

1. Fylingdales, England
2. Thule, Greenland
3. Clear, Alaska
4. Eglin AFB, Florida
5. Diyarbakir, Turkey
6. Shemya, Alaska
7. Canton Island
8. Ascension Island
9. Guam

The tropospheric effects on radio waves include time delay and angular bending. The angular bending or the deviation of the ray path from a straight line is due to the variability of the refractive index of the atmosphere with height above the surface. The net result is generally an apparent target position higher in elevation angle than the true target; that is, the radar wave is bent towards the surface of the earth. The time delay is produced primarily by the index of refraction of the lower atmosphere being slightly greater than unity and to a lesser extent by the lengthened path resulting from the angular bending. This time delay causes the apparent target to be greater than the true range. Figure 1 indicates, in an exaggerated sense, the path of a typical radar wave affected by the lower atmosphere. At elevation angles lower than 10°, the tropospheric refraction effects increase rapidly as seen in Figure 2. As satellite surveillance and tracking demands increase, radars are forced to operate at these very low elevation angles. Figure 2 represents typical refractive effects on a radar wave traveling from the surface to a target in space. The range error in Figure 2a is a one way error; normal radar operation would result in the received signal traversing the atmospheric path twice. Note that the range error varies from about 100 m at 0° elevation angle to about 2.5 m at 90° elevation angle. In addition, the low elevation angle difficulties are evident, with the range error at 10° less than 15 m, while at 5° the range error is almost doubled to 25 m. Figure 2b provided an indication of typical angular bending for a radar wave from the surface to a target in space. Again, note the problem working at elevation angles below 10°. Bending at an elevation angle of 90° is 0°, at 10° about 0.1°, at 5° about 0.2° and at 0°, the bending is close to 0.9°. The results shown in Figure 2 are typical, but do not necessarily represent any of the SPADATS radar site conditions. The data are presented to indicate the approximate magnitude of tropospheric refraction errors that can be expected; actual bending angle and range errors for any of the nine radar sites can be as much as a factor of two larger or smaller than the data presented in Figure 2.

The report is organized into six sections including this introductory section. Section 2 provides a description of the approach taken to satisfy the ESD request.

The computation procedure used to develop the data base used in the final site analyisis is presented in Section 3. Section 4 includes the numerical analysis of the data base including the statistics of the expected tropospheric range error and angular bending for each site. The proposed correction algorithms and an error analysis using these algorithms for each site are presented in Section 5. Conclusions and recommendations are provided in Section 6.

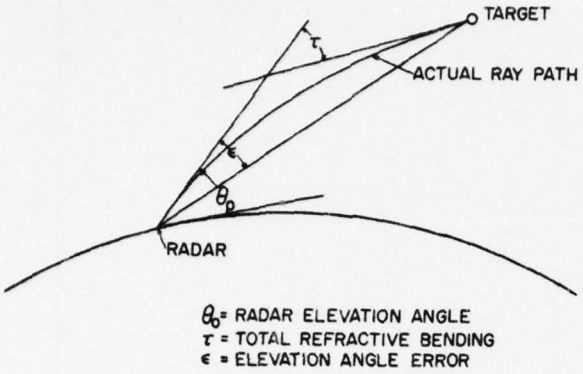


Figure 1. Radar Path Geometry

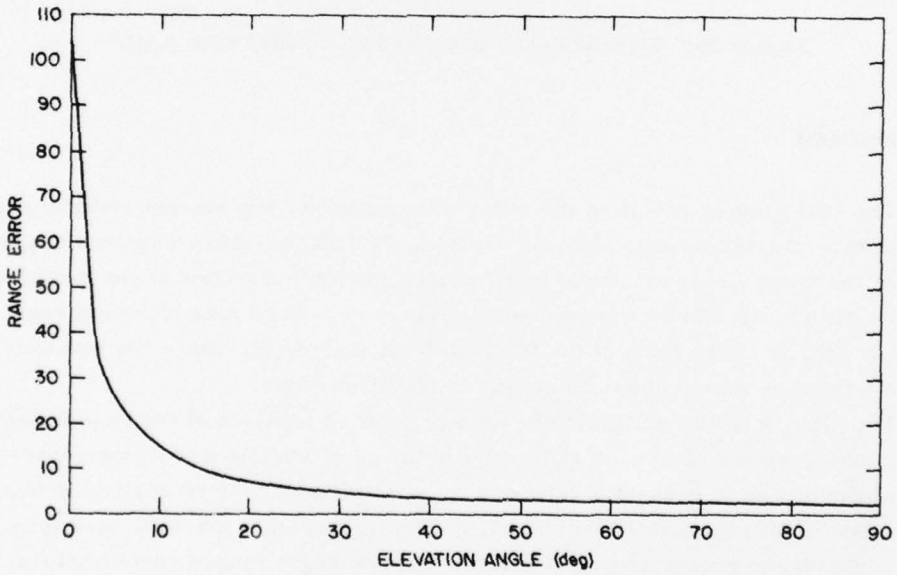


Figure 2a. Typical Range Error vs Elevation Angle

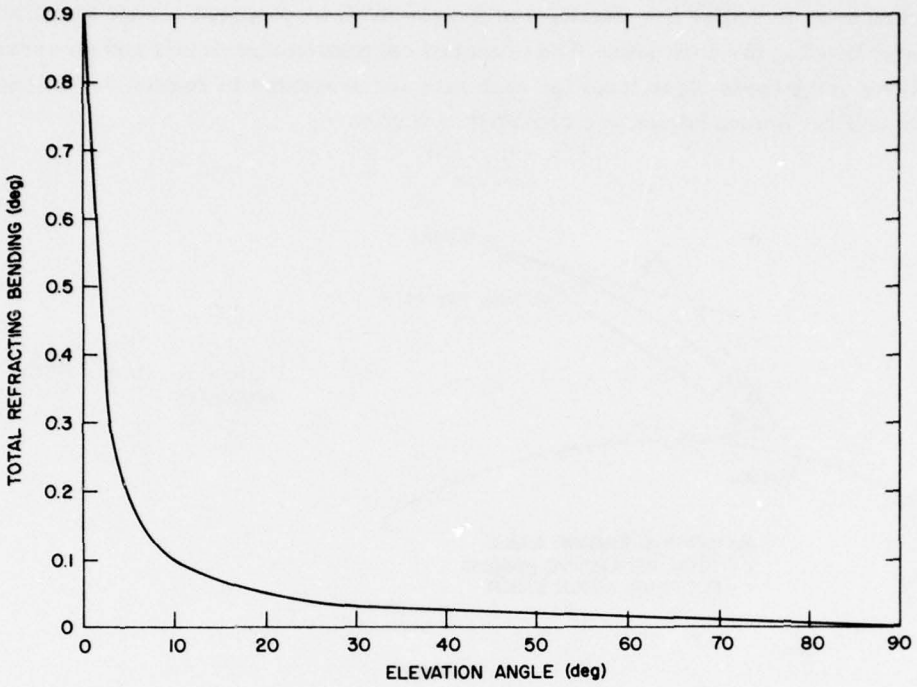


Figure 2b. Typical Refractive Bending vs Elevation Angle

2. APPROACH

The ESD request specified the radar site locations, but was not specific regarding the type of tropospheric analysis desired, the final accuracy required in predicting the range error and angle bending, and the total elevation angle range that the correction algorithms were to be accurate over. The lower elevation angle limit is critical to the form of the final correction algorithm since the major changes in the refractive terms occur below 10° in elevation angle.

The main objective of this study is to present an analysis of the tropospheric environment surrounding each radar site in terms of statistics of range errors and angle bending and to present a selection of correction techniques applicable to each site. The errors associated with each correction technique are evaluated for each site. In order to encompass all possible elevation angle ranges envisioned for each radar site, the decision was made to evaluate tropospheric refraction errors at elevation angles from 0° to 90°. This wide range was chosen even though some of the current radar systems do not operate below 2°, since future installations may allow operation down to an elevation angle near the horizon. Although the impact

of using elevation angles down to 0° on the final correction algorithm was small, it should be emphasized that better correction algorithms can be provided by restricting the analysis to angles above, for example 2°. The use of the entire 0° to 90° range results in a somewhat more complicated expression in the final algorithm than would be needed if the elevation angle range were reduced and the same accuracies were desired. The final form of the correction algorithm will be presented in Section 5.

A fundamental limitation to any tropospheric refraction study, regardless of the level of sophistication of data analysis that is applied, is the accuracy of the data used as input to the study. This limitation is always significant due to the complexity of the tropospheric environment surrounding a given site and the extremely limited sampling of this environment that is currently possible. Ideally, a complete analysis requires a three dimensional representation of the atmosphere with dimensions of about 30 km in height, 100 km in width and 1000 km down range from the radar and this three-dimensional representation should be updated every 30 minutes. However this ideal situation does not exist and probably never will. Current technology ranges from sampling at high resolution using an airborne refractometer to the once or twice a day Rawinsonde launches. The airborne refractometer provides a highly accurate refractive index profile, but only along the particular flight path chosen and the profile is only valid at the time it is taken. The Navy has attempted to measure the highly complex refractive environment on the West coast of the United States with a concentrated airborne refractometer data collection program, but this type of effort is costly and rarely used. The most common source of data is the regularly scheduled Rawinsonde launches which normally occur at 0000Z and 1200Z at over 700 stations in the Northern hemisphere and at several hundred stations in the Southern hemisphere. The limitations of the Rawinsonde data are threefold: the launching sites are generally too widely spaced with separations of 75 to 100 km even in the densely instrumented United States; the launches are widely spaced in time, that is, 12 or 24 hrs and; the sensors used in the Rawinsondes are relatively inaccurate, particularly the humidity sensor. The first limitation means that horizontal variations in the tropospheric refractive structure of less than 100 km will be masked. Horizontal variations in the lower 2 km of the atmosphere are mesoscale in nature and can be significant over distances of less than 10 km. The second limitation has two problems; first, the wide spacing in time and second, the regular launch times. Two Rawinsonde launches per day cannot characterize the atmosphere over the entire 24-hr period. Because of the regular launch times, atmospheric phenomena that occur on a daily basis at certain locations, such as the early morning ducting conditions at Eglin AFB, Florida, are either regularly missed or regularly sampled. Again, the limited sampling does not give a true representation of the atmosphere over a 24-hr period. The third

limitation has a large effect in areas where significant layering of humidity or temperature occurs. The slow response of the humidity sensor effectively smooths the fine detail which actually exists and may entirely miss layers which can lead to the occurrence of ducting. In spite of these fundamental limitations, we are forced to use Rawinsonde data because they are the only data available in significant quantities. All of the results and analyses that follow are presented with the caution that the limitations discussed above are always present. Particular caution must be exercised for elevation angles below 10° since the tropospheric refraction errors are much less sensitive to Rawinsonde data errors for elevation angles above 10°.

The horizontal variations in the tropospheric index of refraction become important at elevation angles below 10° because the atmosphere directly over a radar site is not the same as the atmosphere 50 or 100 km downrange. For a radar operating at a 10° elevation angle, the radar wave passes through an altitude of 4 km at a range of 23 km; for an elevation angle of 3° the 4 km height range is 70 km; for a 1° elevation angle the 4 km height range is 150 km and at an indicated elevation of 0° the 4 km height range is 270 km. The majority of the effects of the troposphere on a radar wave occurs below an altitude of 4 km and the previous data indicates that the 4 km height can be a considerable distance from the radar site. The effects of horizontal variations on tropospheric refraction effects have been reported by Gallop and Telford,[2] Zanter et al,[3] and Vickers and Lopez.[4] Each of these three papers indicate that errors due to horizontal variations are of the same magnitude as the expected errors in predicting refractive range error and angular bending at elevation angles below 10°. The methods used by Gallop and Telford, and Zanter to account for the horizontal variability involved two-dimensional ray tracing using selected sites with Rawinsonde launching stations located within 50 to 100 km of each other. Effective two-dimensional ray tracing requires both a considerable amount of computer time and also requires Rawinsonde stations which are located close together. Since the majority of the radar sites in this report are located in remote areas with widely spaced Rawinsonde stations, the following analysis is performed in one dimension only.

Two years of Rawinsonde data for each primary radar site plus available Rawinsonde sites surrounding the primary sites were used for this analysis. The

2. Gallop, M.A., and Telford, L.E. (1975) Use of atmospheric emission to estimate refractive errors in a non-horizontally stratified troposphere, Radio Sci. 10(No. 11):935-945.

3. Zanter, D.L. et al (1976) The Effect of Atmospheric Refraction on the Accuracy of Laser Ranging Systems, NASA-CR-146313.

4. Vicker, W.W., and Lopez, M.E. (1975) Low angle radar tracking errors induced by nonstratified atmospheric anomalies, Radio Sci. 10(No. 5):491-505.

separation of the secondary sites from the primary sites varied from 130 km to 1250 km. Since the primary and secondary site Rawinsondes are launched at the same time, comparison of calculated range errors and angular bendings from the primary and secondary site profiles will provide an estimate of the impact of horizontal variability.

The final selection of primary and secondary sites are listed in Table 1. Note that Guam and Ascension Island are sufficiently remote such that no secondary sites exist.

Table 1. Primary and Secondary Site Locations

Radar Site	Primary Site		Secondary Site	
1. Fylingdales, England	Aughton, England	53.47N, 02.92W	Shanwell, England	56.43N, 02.87W
			Hemsby, England	52.68N, 01.68W
2. Thule, Greenland	Thule, Greenland	76.52N, 68.84W	Resolute, NWT	74.82N, 94.98W
			Alert, NWT	82.50N, 62.33W
3. Clear, Alaska	Fairbanks, Alaska	64.82N, 147.87W	McGrath, Alaska	62.96N, 155.62W
			Yakutat, Alaska	59.52N, 139.67W
4. Eglin AFB, Florida	Eglin AFB, Florida	30.48N, 86.52W	Montgomery, Alabama	32.30N, 86.40W
5. Diyarbakir, Turkey	Diyarbakir, Turkey	37.92N, 40.20E	Samsun, Turkey	41.28N, 36.33E
			Baghdad, Iraq	33.33N, 44.40E
6. Shemya, Alaska	Shemya, Alaska	52.72N, 174.10E	Adak NS, Alaska	51.90N, 176.65W
			St. Paul Island	57.65N, 170.22W
7. Canton Island	Canton Island	02.80S, 171.6 W	Nandi, Fiji	17.75S, 177.45W
			Pago Pago	14.33S, 170.72W
8. Ascension Island	Ascension Island	07.90S, 14.45W		
9. Guam	Guam	14.96N, 144.80E		

The Rawinsonde data supplied in magnetic tape form by the U.S. Air Force Environmental Technical Applications Center (USAFETAC) consisted of a dump of the raw archived data as received from the field Rawinsonde stations. The conversion of these data into usable form presented a formidable problem which will be discussed in more detail in Section 3. Using the converted Rawinsonde data, range errors and angular bendings were calculated and stored to form the data base for analysis. Statistics of each parameter were compiled and listed for each site. Correction algorithms were derived and tested with an error analysis for each site provided as a final product.

3. COMPUTATION OF DATA BASE

The original data tapes, as supplied by USAFETAC, contained two years of data (1969 and 1970) for 22 stations. Since the data actually consisted of the raw archived data as received from the field, several types of errors existed in the data which had to be removed to assure the best possible accuracy in the analysis. The magnitude of the Rawinsonde data, over 16,000,000 characters, made it imperative that some form of computer error checking be used.

Each profile consisted of data encoded in the universal World Meteorological Organization format which required several computer routines to convert the five character blocks to height, pressure, temperature and dewpoint depression. Temperature data, given in Celsius, suffered from spurious sign changes which greatly affected the ray tracing program used later on in the analysis. The final solution to this problem was to check each temperature against an adopted "standard" profile which discriminated against gross temperature errors. Levels found to have gross temperature errors were corrected by replacing the erroneous temperature with a value interpolated from the nearest valid levels. The raw data were organized into mandatory levels, that is, levels at standard pressures such as 1000 mb, 850 mb, 500 mb, and so on, which had measured heights associated with each level and significant levels, that is, levels that met certain meteorological criteria, which had pressures but no heights associated with them. The significant level data had to be interleaved with the mandatory level data and the significant level heights calculated using the hypsometric equation. Finally, a significant number of profiles had invalid surface data, missing surface data, or less than five levels of data which the conversion routines had to test for and eliminate. After completing all of the above error testing, correction and elimination of invalid data, 79 percent of the original profiles or a total of 19,652 profiles for 22 stations were used as the master profile data base. This represents an average of 893 profiles per station compared with a maximum expected (2 profiles per day) $\times$ (730 days) = 1460 profiles Using 79 percent figure for valid profiles would give an expected

value of (0.79) × (1460) = 1153 profiles per station. The difference between 1153 and 893 profiles per station is due to the fact that several Rawinsonde stations launched only one Rawinsonde per day during most or all of the two-year period and one station missed entire months of data. The final profile count will be discussed within the individual station paragraphs of Section 4.

The master profile data base now contained corrected atmospheric data consisting of pressure, temperature and dew point as a function of height above sea level. Since one of the goals of this study included the analysis of horizontal variations in the troposphere and the approach selected was to look at simultaneous Rawinsonde launches from each primary site and its associated secondary sites, the master profile data base had to be sorted accordingly. A complex sorting routine was devised to arrange each primary site and its associated secondary sites so that simultaneous launching times were grouped. Where several secondary sites were available, various combinations of secondary site profiles were allowed as long as a primary site profile was available. This flexible sorting prevented the absence of any one secondary site from eliminating the entire observation time, however, at least one secondary site profile was required to exist for each available primary site profile. Out of a maximum of 1460 available primary site profiles for the 2-yr period, this sorting procedure produced from 450 to 1395 primary-secondary combinations. Three primary sites, Diyarbakir, Canton Island, and Ascension Island, launched only one Rawinsonde per day and also missed many days entirely during the 2-yr data period.

The next major step was to convert each profile into a series of range errors and angular bendings. The first part of this process is to convert the atmospheric parameters into refractive index (N), using the following equation:

$$N = (n-1)\times 10^{6} = 77.6\,\frac{P}{T} + 4810\,\frac{e}{T^{2}} \qquad (1)$$

where

n = the index of refraction,
P = pressure (mb),
T = temperature (°K),
e = water vapor partial pressure (mb).

The water vapor partial pressure, e, is not commonly available as a measurable quantity, but can be calculated as shown in Eq. (2).

$$e = (6.11) \times 10^{K} \qquad (2)$$

where

$$K = \frac{TDP \times 7.5}{237.3 + TDP}$$

and

TDP = dew point (°C) .

After calculating the refractive index for each profile level, the average profile consisted of 35 refractive index values with corresponding heights varying from the surface to 30 km. The program used to calculate the tropospheric range errors and refractive bendings is a variation of the program used at the National Bureau of Standards during the 1950's and 1960's. The ray tracing is basically Schulkins method and is documented in Bean and Thayer's CRPL Exponential Reference Atmosphere[5] and Bean and Dutton's classic Radio Meteorology.[6] By using the equations described in the CRPL Exponential Reference Atmosphere, the errors created by the ray tracing program are much smaller than those due to the Rawinsonde inaccuracies. The original 35 level average profile is interpolated, primarily at the low levels, so that the computation criteria of Bean and Thayer are met. The interpolation adds 24 levels so that the final profile contains approximately 60 layers. The interpolation routine also extrapolates the top of the profile so that the target height is always 50 km.

The refractive effects are calculated at 27 elevation angles varying from 0° to 90°. Table 2 is a list of the elevation angles used in the analysis part of this study. Note that over one-half of the angles are below 10°, reflecting the large variations expected at the low elevation angles. The output of the final ray tracing program includes the following parameters for each primary-secondary profile combination:

(a) Surface refractivity for each site,

(b) Range error at each angle for each site,

(c) Total refractive bending at each angle for each site,

(d) Elevation angle error at each angle for each site.

These data are stored on magnetic tape for use in the various site analyses which follow. As an indication of the complexity of the computer programs to accomplish the above procedures, the data conversion program used to convert the raw data to usable profiles contains 540 FORTRAN statements and requires 0.2 sec per

5. Bean, B. R., and Thayer, G. D. (1959) CRPL Exponential Reference Atmosphere, Nat. Bur. Stand. Monograph No. 4.

6. Bean, B. R., and Dutton, E. J. (1966) Radio Meteorology, Nat. Bur. Stand. Monograph No. 92.

profile of CDC 6600 computer time. The ray trace program contains 510 FORTRAN statements and requires 1.0 sec per profile to execute on the CDC 6600. Over 2,000,000 range errors and angular bendings were calculated during the course of this investigation.

Table 2. Elevation Angles Used in Refraction Analysis

Elevation Angle (Deg)	
0.0	12.0
0.3	14.0
0.5	16.0
0.7	18.0
1.0	20.0
1.5	25.0
2.0	30.0
2.5	40.0
3.0	50.0
4.0	60.0
5.0	70.0
6.0	80.0
8.0	90.0
10.0	

4. NUMERICAL RESULTS (Site Statistics)

After calculating a two year sample of range errors and angular bendings for each site, the next logical task is to provide a description of the refraction environment for each site. Basically we are not providing a climatology description in a meteorological sense but are restricting the analysis to statistics of the refractive effects at each site. These statistics represent the magnitude of tropospheric refraction errors that can be expected at each site keeping in mind the data base limitations discussed in Section 2.

Before examining the site statistics in detail, a few introductory comments applicable to all the sites are required. The analysis for each site includes statistics on the following refractive parameters: Range error, total refractive bending and the elevation angle error. The total refractive bending ia a measure of the amount the ray is bent as it travels from the surface to the target which is assumed to be at an altitude of 50 km in this study. The elevation angle error is the actual radar elevation angle error due to the troposphere. The elevation angle error is a function of the target height, however this parameter can be extrapolated to any height greater than 50 km by the correction algorithm discussed in Section 5. The other two parameters are not functions of target height for targets outside of

the atmosphere. Statistics for each refractive parameter at each elevation angle include the mean value, the standard deviation, the minimum parameter value and the maximum parameter value for the 2-yr sample. In general, the 2-yr sample includes over 1000 data points, with the exception of Diyarbakir, Canton Island and Ascension Island which have about 500 data points. To test for year-to-year variations, the site statistics were calculated for each year separately. The mean and standard deviation were essentially the same in each year, but the maximum and minimum values were usually somewhat different since these extreme values represent rare non-standard conditions. The site statistics calculated for the available 2-yr data sample represent a valid data set which should be applicable for any 2-yr period assuming no drastic weather pattern changes occur.

The site difference statistics were calculated in an attempt to provide information about the horizontal inhomogeneity of the lower troposphere. At best, these data only provide an upper bound to the effect of horizontal refractive variations on the range error and refractive bending error since the secondary-to-primary site spacings were larger than desired. For elevation angles above 3°, the radar wave passes out of the critical lower portion of the troposphere at a distance of approximately 50 km or less down range from the primary site. Since the primary-to-secondary site spacings are all greater than 100 km, site difference statistics will be restricted to elevation angles below 3°. The master data base was set up to include simultaneous Rawinsonde launches from the primary sites and at least one secondary site. By examining the differences in range error and refractive bending between primary-secondary site pairs for each elevation angle, the same type of statistics listed earlier for the primary sites can be calculated. However, in this case, the mean difference is somewhat biased since slight differences in site elevation will result in different mean parameter values for each site. The critical value is the rms variation of the refractive parameter differences, as this provides a measure of the variability between the two sites on a day to day basis. If the atmosphere over each site were identical each day, the rms variation of the difference of each refractive parameter would be zero while the mean difference could be non-zero due to a height difference. Because of the relatively large primary-to-secondary site spacing, the calculated refractive parameter differences would be expected to be larger than those actually experienced by a low elevation angle radar wave; hence the statistical difference data presented for each site have to be considered an upper limit. Individual site configurations will be discussed as part of the data presentation which follows.

4.1 Fylingdales, England

The Fylingdales data set includes the Aughton, England Rawinsonde site which is very near the radar site plus Hemsby, England which is 130 km southeast of Fylingdales and Shanwell, England which is 350 km due north of Fylingdales. The Hemsby-Fylingdales separation is the closest of any primary-secondary site pair included in this study. Fylingdales and Shanwell are located relatively near the English seacoast while Hemsby is located well inland. Of the possible 1460 profile combinations, 1230 passed the site pairing and data validation tests.

The Fylingdales site statistics listed in Table 3a are representative of a northern midlatitude site with moderate surface refractivity variation and relatively small variations in range error and refractive bending. For example, the range error rms variation at 1° elevation angle is only 20 percent of that at Eglin AFB, Florida and the refractive bending rms variation is 30 percent of the Eglin variation. Comparing Fylingdales to data measured at the RADC Prospect Hill Millimeter Wave Site in Waltham, Massachusetts, the rms variation in refractive bending at Fylingdales is 50 percent of the Prospect Hill variation. In general, the Fylingdales refractive parameter variations are among the lowest of nine radar sites studied. The minimum and maximum refractive parameters also reflect the moderate conditions at Fylingdales. For example, the range error extremes at an elevation angle of 1° are a minimum of 65 m and a maximum of 74 m which is only a 9-m spread.

The difference statistics in Table 3b also indicate the moderate conditions described above. Even though the two primary-secondary site spacings are considerably different, the difference statistics are almost identical. The rms variations of the differences which represent the best measure of the horizontal variability, are close to or less than the rms variations of each site refractive parameter. For precise corrections at elevation angles below 3°, these data represent an upper bound on the errors to be expected due to horizontal variations in the lower tropospheric refractive index.

Ducting seems to be almost non-existent in the Fylingdales data sample. Seven percent of the profiles caused ducting at 0° elevation and no ducting occurred at 0.3°. The data base caution has to be repeated here, since the profiles only represent two regularly timed samples per day and cannot characterize the entire 24-hr day.

4.2 Thule, Greenland

The Thule data set includes two secondary sites; Alert, Northwest Territories which is 675 km north of Thule and Resolute, Northwest Territories which is 750 km west of Thule. The secondary site spacing is much larger than desired for a

horizontal variability test, but obviously, Rawinsonde launching sites are scarce in the north polar region. Of the possible 1460 profile combinations, 1300 sets were analyzed.

The Thule site statistics listed in Table 4a are representative of a continental polar site with small variations in the surface refractive index and relatively small refractive parameter variations. The rms variation of the range error and the refractive bending at an elevation angle of 1° are the smallest of the nine primary radar sites. Interestingly, the peak-to-peak range error at the 1° elevation angle is 24 m which is twice as large as the Fylingdales spread while the rms variation is smaller at Thule. The minimum and maximum are the smallest and largest of any given parameter found over the two-year data sample and evidently the Thule data set has a few extreme profiles while Fylingdales has a consistent spread in profile results.

The site difference statistics are not as relevant as in the case of the other sites due to the wide spacing. Looking at the individual secondary site statistics, which have not been included in this report, the Alert data has more variability than either Thule or Resolute and it is much closer to the North Pole. The difference statistics indicate a different climatology over Alert than exists at the other two sites. The rms variability of the Thule-Alert pair exceeds the rms variations of the Thule data by a factor of two while the Thule-Resolute rms variations are comparable to that of Thule alone. For all practical operational purposes, the Thule site difference data can be disregarded since the rms variations are so small to begin with and the variability between the widely spaced sites is also small.

Ducting phenomena are not a factor at Thule based upon the profiles analyzed. Less than 2 percent of the profiles indicated ducting at 0° elevation angle and no ducting occurred at higher elevation angles. Previously published data have indicated that polar sites can be subject to frequent ducting at certain times of the year due to temperature inversions near the surface. The 0000Z and 1200Z launch times may not coincide with the time of the day when these inversions occur and therefore the 2 percent ducting figure may be low. Based on the presently available data we cannot make a meaningful assessment of the true ducting percentages.

4.3 Clear, Alaska

The Clear data set include Fairbanks, Alaska as the primary site, McGrath, Alaska which is about 340 km southwest of Clear and Yakutat, Alaska which is 725 km southeast of Clear. The Fairbanks Rawinsonde station is 30 km north of Clear. The site spacing is not ideal, since Rawinsonde launching sites are widely scattered in this area. 1060 profile combinations out of a possible 1460 were converted from the master profile data tape.

The site statistics are presented in Table 5a. The Clear site is a continental polar location and is well inland away from the influence of the ocean. The surface refractive index is comparable to that in the northern continental United States and the rms variation of the surface refractivity is relatively high compared to the Thule data. The larger variation is primarily due to the wide variation of surface temperature during the year at Clear. The rms variability of the range error is twice as large as the Thule range error variability and the angular bending variations are one-half again as large which indicates the difference that can exist between the two site environments, even though they are both considered polar continental sites.

The site difference statistics in Table 5b indicate a larger horizontal variability than most of the other sites. As an example of the non-homogeneous tropospheric structure in Alaska, the rms variability of range error difference for the closer pair of sites is greater than the corresponding variability for the wide spaced pair while the variability of the angular bending is just the opposite. The rms variability of each site difference refractive parameter is greater than the individual size variabilities, indicating a definite horizontal inhomogeneity over the relatively large site spacing. In any event, the site spacing is large, even in the case of the closer pair and the site difference statistics have to be considered upper limits on the error due to horizontal variability. A practical horizontal variability error would be one-half the listed rms variabilities at a 1° elevation angle and less than one-half the listed value for higher elevation angles. Above 3°, the horizontal variability error can be neglected.

Ducting occurred in 9 percent of the profiles analyzed at Clear for 0° elevation angle. No ducting was observed at 0.3° and above in the profiles analyzed. The 9 percent ducting figure may be artificially high since close examination of the Rawinsonde data indicated certain profiles with dew points which were arbitrarily set 50°C below the air temperature for the surface readings. Offsetting this problem somewhat is the fact that in these cases, air temperatures were lower than -20°C and the dew point data are suspect at these temperatures. From a refraction point of view, the dew point, when the air temperature is -30°C or below, has little effect on the refractive index. Several of the ducting cases which occurred in the month of January had the 50°C anomaly and the cold air temperatures associated with that problem. A complete check of the entire year was not done, however the effect of this anomaly should be less than 3 percent based upon the profiles checked. The regular caution of the limitations of the twice per day sampling on ducting analysis is certainly applicable in this case since the two sample times are in early morning and late afternoon.

4.4 Eglin AFB, Florida

The original request for the Eglin data set included Montgomery, Alabama and Burnwood, Louisiana as the secondary sites. Unfortunately, the Burwood data were missing from the final ETAC data submission. Two other problems exist with the Eglin data set; first, the Rawinsonde launching site is 32 km west of the radar site and second, the secondary site location is due north while the radar boresight is due south. The radar azimuth coverage is primarily over water so there is little possibility of obtaining significant Rawinsonde coverage where it is needed. In spite of these site location problems the Eglin data set did result in over 1200 usable profiles out of a possible 1460.

Table 6a presents the statistical breakdown of the Eglin refractive parameter data. Eglin has the greatest variation in the surface refractive index and the greatest variations in range error and angular bending of any of the radar sites analyzed. This large variation is characteristic of a near tropical coastal site with conflicting land and sea air masses. The 32 km separation between the radar site and the Rawinsonde launching site becomes important under this type of atmospheric conditions as small scale horizontal variations are more likely to exist. The Montgomery surface refractivity statistics are essentially the same as the Eglin statistics, but the range error variations are less than one-half as large as the Eglin variations. In contrast to this, the angular bending statistics of the two sites are very similar. The angular bending through an atmosphere is a function of the gradient of the refractive index, while the range error is a function of the integral of the refractive index along the ray path. The land-sea interface seems to present more variations in the integral of the refractive index than the inland site while retaining similar gradients near the surface.

Eglin and Montgomery are 200 km apart and the site difference statistics reflect the large separation as well as the coastal vs inland distinction. Looking at the 1° elevation angle data in Table 6b, the mean difference is the difference in the mean values of the refractive parameters while the rms variability of the differences is comparable with the Eglin site rms variations which are large. The Eglin-Montgomery comparison may have some relation to the actual Eglin operational radar paths in spite of Montgomery's inland location. Refractive bending data have been collected for several years at the RADC Prospect Hill Millimeter Wave site. These data consist of measurements at elevation angles between 0° and 20.0° over two paths, one predominantly over water and the other over land. Analysis of 300 over water paths and 300 over land paths indicate essentially identical statistics for each path. Therefore, it is reasonable to expect similar results if the over water path data at Eglin could be compared with the Eglin-Montgomery path. Based on this assumption, the difference statistics should represent an upper limit to the

errors due to horizontal refractive index variability since the Eglin-Montgomery spacing is larger than the distance a low elevation angle wave travels through the lower troposphere.

Ten percent of the Eglin profiles produced ducting at 0° elevation angle and less than 2 percent of the profiles had ducting at an elevation angle of 0.3°. As a comparison, the Montgomery profiles produced 6 percent ducting at 0° and 1 percent at 0.3°.

4.5 Diyarbakir, Turkey

The data set for Diyarbakir presented a unique problem. The altitude of the Diyarbakir Rawinsonde site is 677 m above sea level while the two secondary sites, Samsun, Turkey at an altitude of 44 m and Baghdad, Iraq at an altitude of 34 m are much closer to sea level. In addition, Samsun is 480 km northwest of Diyarbakir and Baghdad is 615 km southeast. The large altitude difference was compensated for by interpolating the secondary site profiles so that only the portion of their profiles above 677 m was used to generate the refractive parameters. Since the Diyarbakir Rawinsonde site only launched one balloon per day and missed blocks of days during the two years, only 460 profile combinations were available out of a possible 1460.

The mean surface refractivity at Diyarbakir is low, reflecting the high altitude location, but the rms variability is relatively large. Our initial expectation was that the variation of the refractive parameters would be small, however the data dispels this. While the variations are not as large as Eglin's, the angular bending rms variability is close to that at Eglin and the range error variability is 40 percent of that at Eglin. The secondary site range error variations are close to the Eglin range error variations indicating a complex and variable refractive environment in the Turkey locations. Table 7a indicates the magnitude of the Diyarbakir site statistics. The 1° elevation angle range error spread is 35 m which is an indication of the variability of the tropospheric environment around Diyarbakir. The 1° elevation angle range error spreads at Samsun and Baghdad are 42 m and 95 m respectively which reinforces the concept of a complex tropospheric refractive environment.

Table 7b contains the site difference statistics and the mean differences are relatively large, indicating that the interpolation process to bring the secondary site altitudes up to the Diyarbakir altitude was not particularly successful; also the rms variabilities of the refractive parameters are the largest of any primary-secondary site pairs analyzed. Even taking into account the relative large site spacing, the horizontal variability is going to affect low elevation angle tropospheric refractive corrections at this site.

Keeping in mind that only 0000Z observations were available, 6 percent of the profiles indicated ducting at 0° elevation angle and 2 percent indicated ducting at 0.3°. These percentages could change if the 1200Z data were available for this analysis.

4.6 Shemya, Alaska

The Shemya data set includes Adak, Alaska and St. Paul Island as the secondary site locations. Adak is 650 km west of Shemya and St. Paul Island is 1200 km northeast of Shemya; both sites being the closest available Rawinsonde stations in the Shemya area. The large spacing again limits the usefulness of the site difference data and in addition, the two secondary sites are in the opposite direction to the normal operating azimuths at Shemya. The Shemya profile data had more uncorrectable data than the other sites resulting in 932 profile combinations out of a possible 1460.

The Shemya site statistics in Table 8a reflect the polar location of the site with a small surface refractivity variation and relatively small refractive parameter variations. The angular bending variation at an elevation angle of 1° is one-half that measured at the RADC Prospect Hill Millimeter Wave Site and the range error spread at 1° is only 8 meters.

The site difference data in Table 8b are interesting because in spite of the very large site spacings, the difference rms variabilities are smaller than the individual site parameter rms variabilities. At least during the time of the twice daily Rawinsonde launches, the horizontal variability in the Shemya area is small. The general location of the three sites is basically open ocean with no nearby land mass to create horizontal variations and the very dry atmosphere removes the water vapor variability. Even at the low elevation angles at which the Shemya based radars operate, errors due to horizontal variations in the troposphere will be negligible.

Approximately 9 percent of the profiles analyzed had ducting at 0° and no ducting occurred at 0.3° or above. This agrees well with an independent ETAC study using four different years of Rawinsonde data which found 10 percent ducting at 0°. The usual caution about the limited Rawinsonde sample time has to be repeated since actual ducting conditions could exist at times other than the 0000Z and 1200Z launch times. The 9 percent ducting at 0° is larger than the ducting percentage at the other polar sites analyzed.

4.7 Canton Island

The Canton Island site is in a South Pacific location which classifies it as an Isothermal-Equatorial climate type with a high average surface refractive index with little variation in the refractive index. The two secondary sites are Nandi in the Fiji Islands and Pago Pago which are 2000 km and 1300 km, respectively from Canton Island. Obviously these large site spacings make any site difference statistics academic, however the data will be included for completeness. The Canton Island data sample covers two consecutive years, however only 0000Z Rawinsonde launches were included in the data supplied by ETAC. Therefore, only 537 profile combinations are available for analysis.

Table 9a contains the statistical site data for Canton Island. The average surface refractivity at Canton Island is among the highest of all the sites analyzed, however, the rms variability is not large. This is consistent with equatorial site climatology. Corresponding to this high mean surface refractive index are relatively high mean range errors and refractive bending. For example, at an elevation angle of 1°, the mean Canton Island total refractive bending is 0.689°, compared to 0.559° at Eglin and 0.487° at Prospect Hill. However, the rms variability of the same parameter at Canton is only 0.046°, compared to 0.060° at Eglin and 0.057° at Prospect Hill. Another interesting comparison is the relative variation of the refractive bending and the range error. The range error variability at Canton Island is comparable to the northern latitude sites while the refractive bending variability is twice as large. This is indicative of large gradient changes near the surface since the refractive bending is sensitive to surface level gradients of the refractive index while the range error is not. This gradient variation is also supported by the extremely high ducting percentage for low elevation angles at Canton Island. Eighty percent of the available profiles had ducting at 0° elevation angle, 28 percent at 0.3° and 3 percent at 0.5°. This is the highest percentage of ducting found at any of the primary or secondary sites. The 0000Z time at Canton Island corresponds to approximately noon local time and the ducting is primarily caused by the high humidity marine layer that is approximately 150 m thick and is surfaced based at that time. From a meteorological point of view, the marine layer will persist during the night time hours and will usually intensify after sunset due to the relatively warm sea surface. Since the island is low and surrounded by the ocean, the marine layer will exist over the radar site if the site is below about 100 m above sea level and the high percentage of ducting can be expected to exist both day and night.

As stated earlier the site difference statistics are academic because the site spacings are so large. This large spacing is apparent in the large variability in the difference data. The range error variability is relatively small compared to the refractive bending variability. The actual profile data for the three sites reveal that the Canton Island site is the only one to have the persistent humid marine layer which would lead to large gradients and gradient changes near the surface. This is consistent with the large variability in the refractive bending difference data.

4.8 Ascension Island

The Ascension Island data set includes only the primary site as there are no other Rawinsonde sites within any reasonable distance. In addition, only one launch per day at 1200Z was available in the ETAC data archives. As a result, only 500 profiles are available for analysis for the two-year period and no site difference data are presented.

The Ascension Island statistics are presented in Table 10. The site generally has a moderate mean surface refractive index of 358 N-units with a relatively low rms variability. The refractive parameter variations are comparable to the surface refractive index with relatively high mean values and relatively low variations. For example, at an elevation angle of 1°, the range error is spread only 12 meters.

Only 3 percent of the profiles indicated ducting at 0° elevation angle and no ducting was detected at higher elevation angles. The once per day Rawinsonde occurs approximately at noon local time and it is not clear whether this low ducting percentage would continue into the nighttime hours.

4.9 Guam

The Guam data base is similar to that of Ascension Island in that only primary site data are available, however two soundings per day were provided. The quality of the primary site data was above average and 1355 profiles were used out of the possible 1460. Since no secondary site data were provided, no site difference statistics are presented.

The Guam mean surface refractivity is the highest of any site analyzed, however the rms variability was the lowest which is typical of an Isothermal-Equatorial climate. The refractive parameters reflect the surface conditions with generally high mean values and relatively low rms variations. The range error spread is 13 m and the refractive bending spread is 0.300°.

The ducting percentage is 13 percent at 0° elevation angle and no ducting is found at 0.3° and above indicating a shallow duct with only marginal ducting gradients. The data base did include both daytime and nighttime launches so the ducting percentages are probably representative of the entire day.

Table 3a. Fylingdales Site Statistics. (Mean surface refractivity 324.8, rms variability of surface refractivity 21.9)

Elevation Angle (deg)	Range Error (m)				Total Refractive Bending (deg)				Elevation Error (deg)			
	Min	Max	Mean	rms	Min	Max	Mean	rms	Min	Max	Mean	rms
0.0	95.3	179.5	113.4	9.6	0.450	1.970	0.912	0.176	0.304	1.633	0.724	0.155
0.3	85.6	106.8	93.2	3.3	0.493	1.064	0.708	0.060	0.360	0.892	0.560	0.054
0.5	78.6	93.1	84.3	2.6	0.485	0.803	0.636	0.044	0.362	0.655	0.504	0.039
0.7	72.5	83.7	77.1	2.1	0.465	0.703	0.580	0.036	0.352	0.575	0.461	0.032
1.0	64.5	73.1	68.2	1.7	0.431	0.601	0.513	0.028	0.331	0.490	0.410	0.025
2.0	46.2	51.9	48.7	1.0	0.329	0.414	0.368	0.016	0.260	0.341	0.299	0.025
5.0	23.8	29.9	25.1	0.5	0.175	0.663	0.192	0.015	0.144	0.624	0.160	0.015
10.0	12.8	15.2	13.5	0.3	0.094	0.324	0.102	0.007	0.079	0.306	0.086	0.007
20.0	6.6	7.7	7.0	0.1	0.047	0.157	0.051	0.003	0.039	0.148	0.043	0.003
60.0	2.6	3.0	2.8	0.1	0.010	0.033	0.011	0.001	0.008	0.031	0.009	0.001
90.0	2.3	2.6	2.4	0.05	0.000	0.000	0.000	0.000	0.000	0.000	0.000	0.000

Table 3b. Fylingdales Site Difference Statistics

Shanwell

Elevation Angle (deg)	Range Error Difference (m)				Total Refractive Bending Difference (deg)			
	Min	Max	Mean	rms	Min	Max	Mean	rms
0.0	-61.1	56.6	-2.0	10.7	-1.026	0.946	-0.047	0.213
0.3	-11.4	12.5	-0.3	2.6	-0.328	0.322	-0.016	0.063
0.5	- 7.0	13.7	-0.1	1.8	-0.189	0.520	-0.009	0.051
0.7	- 5.6	6.8	0.0	1.3	-0.142	0.232	-0.008	0.035
1.0	- 4.5	6.5	0.0	1.1	-0.102	0.121	-0.006	0.025
2.0	- 3.0	5.1	0.0	0.8	-0.059	0.069	-0.002	0.019

Hembsy

Elevation Angle (deg)	Range Error Difference (m)				Total Refractive Bending Difference (deg)			
	Min	Max	Mean	rms	Min	Max	Mean	rms
0.0	-54.2	69.3	-0.9	11.5	-0.982	1.152	-0.033	0.228
0.3	-10.6	18.0	0.7	2.8	-0.359	0.494	0.006	0.076
0.5	- 7.0	11.7	0.6	1.8	-0.147	0.279	0.006	0.049
0.7	- 5.3	8.1	0.6	1.3	-0.114	0.194	0.005	0.036
1.0	- 3.9	5.7	0.5	1.0	-0.087	0.133	0.004	0.026
2.0	- 1.9	3.0	0.3	0.6	-0.049	0.064	0.003	0.013

Table 4a. Thule Site Statistics. (Mean surface refractivity 308.4, rms variability of surface refractivity 9.1)

Elevation Angle (deg)	Range Error (m)				Total Refractive Bending (deg)				Elevation Error (deg)			
	Min	Max	Mean	rms	Min	Max	Mean	rms	Min	Max	Mean	rms
0.0	91.5	157.9	102.6	6.8	0.438	1.741	0.714	0.150	0.297	1.449	0.550	0.135
0.3	81.0	105.6	87.9	2.5	0.449	1.000	0.611	0.061	0.322	0.845	0.473	0.057
0.5	74.7	99.2	80.4	1.9	0.441	1.051	0.563	0.047	0.323	0.845	0.438	0.044
0.7	69.1	93.2	74.0	1.6	0.427	1.081	0.521	0.039	0.318	0.932	0.408	0.036
1.0	61.9	85.5	65.8	1.3	0.400	0.801	0.468	0.028	0.303	0.684	0.369	0.026
2.0	44.8	67.1	47.3	0.9	0.307	0.492	0.344	0.015	0.239	0.420	0.276	0.014
5.0	23.1	41.1	24.4	0.6	0.165	0.236	0.181	0.006	0.124	0.205	0.150	0.006
10.0	12.4	24.6	13.1	0.4	0.089	0.124	0.097	0.003	0.065	0.108	0.082	0.003
20.0	6.4	13.4	6.8	0.2	0.044	0.061	0.048	0.001	0.032	0.054	0.041	0.001
60.0	2.6	5.4	2.7	0.1	0.009	0.013	0.010	0.001	0.007	0.011	0.009	0.001
90.0	2.2	4.7	2.3	0.1	0.000	0.000	0.000	0.000	0.000	0.000	0.000	0.000

Table 4b. Thule Site Difference Statistics

Resolute

Elevation Angle (deg)	Range Error Difference (m)				Total Refractive Bending Difference (deg)			
	Min	Max	Mean	rms	Min	Max	Mean	rms
0.0	-49.7	66.1	3.1	7.9	-0.946	1.190	0.062	0.173
0.3	-18.4	12.0	2.0	2.5	-0.375	0.325	0.051	0.065
0.5	-19.0	21.0	1.6	2.1	-0.470	0.585	0.043	0.058
0.7	-19.3	11.5	1.1	1.7	-0.520	0.383	0.035	0.044
1.0	-19.6	6.3	0.8	1.3	-0.296	0.309	0.027	0.032
2.0	-19.6	3.5	0.3	1.0	-0.123	0.121	0.015	0.015

Alert

Elevation Angle (deg)	Range Error Difference (m)				Total Refractive Bending Difference (deg)			
	Min	Max	Mean	rms	Min	Max	Mean	rms
0.0	-35.7	77.2	3.5	8.1	-0.764	1.169	0.068	0.165
0.3	-12.3	75.6	2.2	3.8	-0.405	0.422	0.052	0.074
0.5	-16.4	74.9	1.6	3.3	-0.486	0.581	0.042	0.066
0.7	-16.5	74.3	1.2	3.2	-0.517	0.884	0.035	0.060
1.0	- 8.6	73.5	0.9	2.9	-0.299	0.868	0.029	0.049
2.0	- 8.7	70.7	0.3	2.5	-0.130	0.287	0.015	0.021

Table 5a. Clear Site Statistics. (Mean surface refractivity 305.0, rms variability of surface refractivity 12.7)

Elevation Angle (deg)	Range Error (m)				Total Refractive Bending (deg)				Elevation Error (deg)			
	Min	Max	Mean	rms	Min	Max	Mean	rms	Min	Max	Mean	rms
0.0	86.2	170.8	103.6	9.8	0.442	1.932	0.765	0.194	0.293	1.611	0.598	0.172
0.3	79.4	98.5	88.2	4.5	0.448	1.106	0.639	0.094	0.324	0.925	0.500	0.086
0.5	72.5	86.6	80.2	3.4	0.436	0.844	0.577	0.064	0.321	0.699	0.452	0.059
0.7	66.6	78.7	73.6	2.9	0.419	0.722	0.529	0.050	0.313	0.596	0.416	0.046
1.0	59.2	69.6	65.4	2.6	0.388	0.609	0.472	0.037	0.287	0.502	0.373	0.035
2.0	42.5	49.7	47.0	2.2	0.278	0.417	0.344	0.020	0.198	0.347	0.277	0.019
5.0	22.0	25.7	24.3	1.7	0.146	0.210	0.181	0.008	0.082	0.178	0.150	0.008
10.0	11.9	14.0	13.1	1.2	0.084	0.111	0.097	0.004	0.033	0.095	0.081	0.004
20.0	6.1	7.3	6.8	0.7	0.043	0.055	0.048	0.002	0.013	0.047	0.041	0.002
60.0	2.4	2.9	2.7	0.2	0.009	0.012	0.010	0.001	0.002	0.010	0.009	0.001
90.0	2.1	2.5	2.3	0.1	0.000	0.000	0.000	0.000	0.000	0.000	0.000	0.000

Table 5b. Clear Site Difference Statistics

Clear-McGrath

Elevation Angle (deg)	Range Error Difference (m)				Total Refractive Bending Difference (deg)			
	Min	Max	Mean	rms	Min	Max	Mean	rms
0.0	-64.6	66.1	-0.5	9.7	-0.978	1.153	-0.019	0.203
0.3	-64.4	11.5	0.0	3.5	-0.362	0.329	-0.007	0.075
0.5	-64.6	11.1	0.2	2.9	-0.229	0.397	0.000	0.050
0.7	-64.7	7.0	0.2	2.7	-0.165	0.235	0.001	0.036
1.0	-64.7	5.8	0.2	2.5	-0.114	0.151	0.002	0.026
2.0	-64.1	3.9	0.1	2.3	-0.060	0.067	0.002	0.013

Clear-Yakutat

Elevation Angle (deg)	Range Error Difference (m)				Total Refractive Bending Difference (deg)			
	Min	Max	Mean	rms	Min	Max	Mean	rms
0.0	-71.3	65.9	4.6	13.0	-1.283	1.177	0.034	0.263
0.3	-59.1	18.2	2.9	5.1	-0.506	0.480	0.033	0.112
0.5	-59.9	33.9	2.6	3.9	-0.288	0.842	0.030	0.080
0.7	-60.5	18.5	2.2	3.3	-0.206	0.526	0.026	0.061
1.0	-61.1	10.9	1.9	2.8	-0.150	0.353	0.021	0.045
2.0	-60.8	6.6	1.2	2.3	-0.078	0.169	0.014	0.024

Table 6a. Eglin Site Statistics. (Mean surface refractivity 342.4, rms variability of surface refractivity 26.5)

Elevation Angle (deg)	Range Error (m)				Total Refractive Bending (deg)				Elevation Error (deg)			
	Min	Max	Mean	rms	Min	Max	Mean	rms	Min	Max	Mean	rms
0.0	93.3	313.7	220.2	19.1	0.464	1.990	0.955	0.270	0.317	1.648	0.754	0.236
0.3	82.6	255.3	99.0	12.0	0.483	1.329	0.774	0.130	0.345	1.125	0.624	0.115
0.5	76.3	231.1	89.3	10.4	0.468	1.108	0.697	0.103	0.349	0.949	0.556	0.091
0.7	70.7	213.8	81.4	9.3	0.441	0.943	0.635	0.086	0.331	0.814	0.509	0.077
1.0	63.5	192.7	71.7	8.1	0.405	0.770	0.559	0.069	0.308	0.070	0.451	0.062
2.0	46.4	140.7	50.8	5.7	0.306	0.490	0.346	0.040	0.242	0.432	0.324	0.037
5.0	24.3	73.7	26.0	2.9	0.165	0.242	0.203	0.017	0.135	0.206	0.170	0.016
10.0	13.0	39.4	14.0	1.6	0.089	0.127	0.108	0.009	0.074	0.110	0.092	0.008
20.0	6.8	20.3	7.2	0.8	0.044	0.063	0.053	0.004	0.037	0.054	0.046	0.004
60.0	2.7	8.1	2.9	0.3	0.009	0.013	0.011	0.001	0.008	0.012	0.010	0.001
90.0	2.3	7.0	2.5	0.3	0.000	0.000	0.000	0.000	0.000	0.000	0.000	0.000

Table 6b. Eglin Site Difference Statistics

Montgomery

Elevation Angle (deg)	Range Error Difference (m)				Total Refractive Bending Difference (deg)			
	Min	Max	Mean	rms	Min	Max	Mean	rms
0.0	-70.9	188.8	6.1	19.1	-1.027	1.330	0.104	0.300
0.3	-32.1	155.4	2.8	10.5	-0.431	0.598	0.054	0.116
0.5	-30.4	142.0	2.0	9.2	-0.291	0.443	0.041	0.080
0.7	-29.0	131.7	1.5	8.4	-0.212	0.334	0.033	0.061
1.0	-26.9	118.6	1.1	8.1	-0.146	0.231	0.024	0.043
2.0	-20.8	88.3	0.5	5.6	-0.069	0.104	0.052	0.021

Table 7a. Diyarbakir Site Statistics. (Mean surface refractivity 289.4, rms variability of surface refractivity 18.6)

Elevation Angle (deg)	Range Error (m)				Total Refractive Bending (deg)				Elevation Error (deg)			
	Min	Max	Mean	rms	Min	Max	Mean	rms	Min	Max	Mean	rms
0.0	83.0	150.7	98.5	9.4	0.414	1.770	0.754	0.201	0.290	1.488	0.595	0.179
0.3	74.0	112.3	83.1	4.9	0.429	1.007	0.614	0.106	0.317	0.855	0.484	0.097
0.5	68.3	105.2	75.6	4.0	0.410	1.189	0.552	0.083	0.300	1.028	0.436	0.077
0.7	63.0	99.2	69.6	3.7	0.364	1.208	0.508	0.086	0.258	1.067	0.402	0.081
1.0	56.4	91.6	61.8	2.9	0.312	0.787	0.447	0.057	0.212	0.684	0.355	0.053
2.0	41.3	72.7	44.7	2.1	0.222	0.459	0.323	0.030	0.135	0.344	0.260	0.029
5.0	21.9	42.4	23.3	1.3	0.137	0.219	0.170	0.012	0.077	0.189	0.140	0.012
10.0	11.8	23.6	12.6	0.7	0.080	0.125	0.091	0.006	0.048	0.100	0.076	0.006
20.0	6.1	12.4	6.5	0.4	0.040	0.037	0.045	0.003	0.026	0.050	0.038	0.003
60.0	2.4	6.9	2.6	0.1	0.008	0.022	0.010	0.001	0.006	0.010	0.008	0.001
90.0	2.1	4.3	2.3	0.1	0.000	0.000	0.000	0.000	0.000	0.000	0.000	0.000

Table 7b. Diyarbakir Site Difference Statistics

Samson

Elevation Angle (deg)	Range Error Difference (m)				Total Refractive Bending Difference (deg)			
	Min	Max	Mean	rms	Min	Max	Mean	rms
0.0	-29.1	45.2	6.4	13.7	-1.125	0.539	-0.194	0.235
0.3	-25.9	42.8	10.5	10.3	-0.573	0.387	-0.086	0.144
0.5	-25.5	40.7	11.2	9.4	-0.657	0.318	-0.050	0.177
0.7	-25.5	38.2	11.0	8.7	-0.739	0.266	-0.034	0.199
1.0	-25.8	35.8	10.6	7.5	-0.370	0.220	-0.012	0.084
2.0	-25.1	30.6	8.1	5.7	-0.164	0.662	-0.010	0.064

Baghdad

Elevation Angle (deg)	Range Error Difference (m)				Total Refractive Bending Difference (deg)			
	Min	Max	Mean	rms	Min	Max	Mean	rms
0.0	-44.9	83.7	6.9	18.4	-1.082	0.524	-0.183	0.212
0.3	-12.5	92.7	10.1	16.0	-0.546	0.530	-0.107	0.142
0.5	- 9.6	90.8	10.9	15.1	-0.379	0.470	-0.072	0.105
0.7	-15.2	86.7	10.8	14.5	-0.705	0.416	-0.058	0.106
1.0	- 6.1	79.2	10.6	13.3	-0.335	0.349	-0.036	0.073
2.0	- 3.8	56.9	8.7	10.0	-0.125	0.214	-0.012	0.040

Table 8a. Shemya Site Statistics. (Mean surface refractivity 314.7, rms variability of surface refractivity 9.1)

Elevation Angle (deg)	Range Error (m)				Total Refractive Bending (deg)				Elevation Error (deg)			
	Min	Max	Mean	rms	Min	Max	Mean	rms	Min	Max	Mean	rms
0.0	91.0	174.1	106.0	7.5	0.409	1.908	0.782	0.149	0.270	1.583	0.610	0.133
0.3	82.4	102.7	90.0	2.9	0.463	1.019	0.657	0.062	0.334	0.853	0.515	0.057
0.5	76.5	87.7	81.9	2.2	0.459	0.753	0.597	0.044	0.340	0.619	0.470	0.042
0.7	70.5	80.2	75.1	1.8	0.443	0.657	0.549	0.035	0.334	0.539	0.434	0.032
1.0	62.8	71.1	66.6	1.5	0.412	0.560	0.489	0.026	0.315	0.457	0.389	0.025
2.0	45.1	51.2	47.8	0.9	0.315	0.386	0.355	0.014	0.249	0.316	0.286	0.013
5.0	23.3	26.4	24.7	0.5	0.170	0.198	0.185	0.006	0.239	0.166	0.154	0.005
10.0	12.5	14.2	13.2	0.3	0.091	0.105	0.099	0.003	0.076	0.084	0.083	0.003
20.0	6.5	7.3	6.9	0.1	0.045	0.052	0.049	0.001	0.038	0.044	0.042	0.001
60.0	2.6	2.9	2.7	0.1	0.010	0.011	0.010	0.001	0.008	0.009	0.009	0.001
90.0	2.2	2.5	2.4	0.05	0.000	0.000	0.000	0.000	0.000	0.000	0.000	0.000

Table 8b. Shemya Site Difference Statistics

St. Paul

Elevation Angle (deg)	Range Error Difference (m)				Total Refractive Bending Difference (deg)			
	Min	Max	Mean	rms	Min	Max	Mean	rms
0.0	-69.1	50.3	-0.4	8.1	-1.181	0.938	-0.009	0.174
0.3	- 9.4	8.1	0.2	2.4	-0.360	0.281	0.002	0.068
0.5	- 5.9	6.2	0.3	1.7	-0.189	0.132	0.005	0.045
0.7	- 4.8	5.6	0.2	1.4	-0.146	0.101	0.005	0.034
1.0	- 3.8	4.9	0.2	1.2	-0.106	0.075	0.005	0.024
2.0	- 2.8	3.2	0.1	0.8	-0.051	0.040	0.003	0.012

Adak

Elevation Angle (deg)	Range Error Difference (m)				Total Refractive Bending Difference (deg)			
	Min	Max	Mean	rms	Min	Max	Mean	rms
0.0	-70.5	66.6	-2.8	8.7	-1.236	1.105	-0.071	0.185
0.3	-11.5	8.3	-0.8	2.5	-0.333	0.155	-0.031	0.070
0.5	- 7.2	6.9	-0.4	1.7	-0.169	0.110	-0.020	0.047
0.7	- 5.6	5.9	-0.2	1.4	-0.131	0.083	-0.014	0.035
1.0	- 4.1	4.9	0.0	1.1	-0.203	0.063	-0.004	0.025
2.0	- 2.6	3.7	0.1	0.8	-0.058	0.040	-0.004	0.013

Table 9a. Canton Island Site Statistics. (Mean surface refractivity 375.1, rms variability of surface refractivity 10.3)

Elevation Angle (deg)	Range Error (m)				Total Refractive Bending (deg)				Elevation Error (deg)				
	Min	Max	Mean	rms	Min	Max	Mean	rms	Min	Max	Mean	rms	
0.0	105.9	184.8	137.2	17.3	0.536	1.933	1.234	0.290	0.346	1.586	0.990	0.253	(Note 1)
0.3	94.2	147.2	113.9	7.5	0.663	1.784	1.126	0.166	0.485	1.513	0.931	0.151	
0.5	84.3	123.8	98.3	5.4	0.672	1.598	0.966	0.143	0.520	1.378	0.803	0.132	
0.7	76.7	104.2	86.5	2.8	0.604	1.435	0.827	0.086	0.486	1.263	0.688	0.083	
1.0	67.7	81.9	74.2	1.8	0.526	0.901	0.689	0.046	0.424	0.784	0.574	0.045	
2.0	48.3	57.6	51.1	1.5	0.370	0.517	0.457	0.018	0.302	0.446	0.383	0.028	
5.0	24.8	29.0	25.9	0.5	0.191	0.244	0.225	0.007	0.159	0.212	0.192	0.007	
10.0	13.3	15.5	13.9	0.3	0.102	0.127	0.119	0.003	0.086	0.121	0.102	0.003	
20.0	6.9	8.0	7.2	0.1	0.050	0.063	0.059	0.002	0.043	0.055	0.052	0.002	
60.0	2.7	3.2	2.9	0.1	0.011	0.013	0.012	0.001	0.009	0.012	0.012	0.001	
90.0	2.4	2.8	2.5	0.05	0.000	0.000	0.000	0.000	0.000	0.000	0.000	0.000	

1 80% of profiles had ducts at 0.0 degrees.

Table 9b. Canton Island Site Difference Statistics

Nande

Elevation Angle (deg)	Range Error Difference (m)				Total Refractive Bending Difference (deg)			
	Min	Max	Mean	rms	Min	Max	Mean	rms
0.0	-70.7	56.3	-8.6	25.7	-1.143	1.179	-0.181	0.437
0.3	-41.2	29.1	-9.3	13.3	-0.992	0.532	-0.276	0.202
0.5	-26.7	11.3	-4.6	7.7	-0.845	0.180	-0.209	0.156
0.7	-16.5	9.7	-1.4	4.1	-0.724	0.224	-0.141	0.097
1.0	- 7.5	7.9	0.4	2.9	-0.292	0.097	-0.088	0.055
2.0	- 5.0	5.2	1.3	1.9	-0.101	0.058	-0.033	0.026

Pago Pago

Elevation Angle (deg)	Range Error Difference (m)				Total Refractive Bending Difference (deg)			
	Min	Max	Mean	rms	Min	Max	Mean	rms
0.0	-69.6	56.0	-7.2	25.3	-1.198	0.924	-0.190	0.433
0.3	-32.1	26.6	-4.4	9.3	-0.738	0.331	-0.204	0.207
0.5	-24.1	21.6	0.6	6.3	-0.872	0.575	-0.096	0.187
0.7	-12.8	13.9	2.0	3.5	-0.698	0.357	-0.058	0.112
1.0	- 4.7	9.5	2.6	2.6	-0.247	0.199	-0.029	0.059
2.0	- 4.0	6.6	2.2	1.9	-0.065	0.105	-0.003	-0.023

Table 10. Ascension Island Site Statistics. (Mean surface refractivity 357.6, rms variability of surface refractivity 12.6)

Elevation Angle (deg)	Range Error (m)				Total Refractive Bending (deg)				Elevation Error (deg)			
	Min	Max	Mean	rms	Min	Max	Mean	rms	Min	Max	Mean	rms
0.0	98.0	165.1	122.0	10.1	0.522	1.698	0.977	0.183	0.361	1.399	0.770	0.161
0.3	90.2	120.4	101.4	4.6	0.604	1.265	0.822	0.092	0.457	1.056	0.654	0.082
0.5	83.5	101.3	91.3	3.2	0.595	1.034	0.746	0.065	0.457	0.861	0.598	0.059
0.7	77.0	91.2	82.9	2.5	0.564	0.842	0.682	0.051	0.441	0.746	0.550	0.046
1.0	68.4	79.7	72.7	1.9	0.511	0.746	0.600	0.038	0.425	0.626	0.488	0.035
2.0	48.7	55.6	51.1	1.1	0.374	0.487	0.421	0.020	0.304	0.413	0.348	0.019
5.0	25.1	28.0	26.0	0.4	0.194	0.237	0.213	0.008	0.162	0.204	0.180	0.008
10.0	13.4	15.0	13.9	0.2	0.103	0.124	0.113	0.004	0.087	0.108	0.097	0.004
20.0	7.0	7.7	7.2	0.1	0.051	0.061	0.056	0.002	0.043	0.053	0.047	0.002
60.0	2.8	3.1	2.9	0.05	0.011	0.013	0.012	0.001	0.009	0.011	0.020	0.001
90.0	2.4	2.7	2.5	0.04	0.000	0.000	0.000	0.000	0.000	0.000	0.000	0.000

Table 11. Guam Site Statistics. (Mean surface refractivity 377.6, rms variability of surface refractivity 8.7)

Elevation Angle (deg)	Range Error (m)				Total Refractive Bending (deg)				Elevation Error (deg)			
	Min	Max	Mean	rms	Min	Max	Mean	rms	Min	Max	Mean	rms
0.0	98.1	190.8	131.8	11.0	0.508	1.974	1.048	0.189	0.355	1.622	0.870	0.166
0.3	88.2	131.7	108.3	3.9	0.521	1.573	0.928	0.081	0.382	1.339	0.746	0.074
0.5	81.2	104.2	96.6	2.7	0.510	1.075	0.830	0.052	0.382	0.913	0.671	0.049
0.7	74.9	92.2	87.1	2.3	0.490	0.904	0.750	0.037	0.373	0.756	0.610	0.035
1.0	66.8	80.2	75.9	2.0	0.455	0.751	0.653	0.026	0.352	0.630	0.535	0.025
2.0	47.5	55.7	52.7	1.4	0.345	0.491	0.451	0.013	0.275	0.415	0.375	0.012
5.0	24.5	28.1	26.6	0.7	0.183	0.239	0.226	0.005	0.151	0.206	0.102	0.005
10.0	13.2	15.0	14.2	0.3	0.098	0.126	0.119	0.003	0.082	0.109	0.103	0.003
20.0	6.8	7.8	7.4	0.2	0.049	0.062	0.059	0.001	0.041	0.054	0.051	0.001
60.0	3.1	3.5	3.3	0.1	0.015	0.019	0.018	0.001	0.013	0.017	0.016	0.001
90.0	2.3	2.7	2.5	0.1	0.000	0.000	0.000	0.000	0.000	0.000	0.000	0.000

5. CORRECTION METHODS AND RESULTS

After completing the site statistics analysis for each site, the development of algorithms to correct for the tropospheric refractive effects was necessary. Past correction methods have ranged from the very simple, involving an expression using just a cosecant term and the elevation angle with a constant refractive index term, to rather complex table generation and look-up operations where real time Rawinsonde data input are available. ESD placed no definitive speed or memory size restrictions on the algorithm, but they were interested in keeping the memory requirements to a minimum and keeping the execution time relatively short, that is, less than 50 msec on a state-of-the-art minicomputer.

The correction algorithms were designed to operate at elevation angles from 0° to 90°. By adopting this wide range of elevation angles, the final algorithm, while not complex, is more complicated than if the lower elevation angle limit were raised to 5° or more. This is because of the large increase in both range error and refractive bending at elevation angles below 5° as shown earlier in Figure 2. The other disadvantage to a complete 0° to 90° elevation angle range is the somewhat degraded fit of the algorithm to the actual data at elevation angles less than 20°. While the final result is more than adequate for the majority of the radar systems used at the selected sites, the algorithm fit could be made better with the acceptance of a restricted elevation angle coverage.

The actual algorithm form that was decided upon was originally formulated by Berman and Rockwell.[7] They were in search of an angular refraction model that would be usable over elevation angles ranging from -5.0° to 90.0° with no discontinuities in the model output. Berman and Rockwell used a statistical approach to develop a model to suit their purpose. The original data source was an optical refractive bending table, with a constant, standard surface pressure and temperature which were known to be very accurate. They attempted to fit an Nth order polynomial to the tabulated data using least squares techniques with less than ideal results. The minimum order polynomial that gave a reasonable fit was of order 12 and the residual errors were unacceptably high near 0° elevation angle. After modifying their model, the following expression, which is not too complex, provided the best fit.

$$\text{BEND} \sim \text{EXP} \left\{ \sum_j K_j \left[U(Z) \right]^j \right\} - C \qquad (3)$$

7. Berman, A.L., and Rockwell, S.T. (1974) A New Angular Tropospheric Refraction Model, The Deep Space Network Progress Report, No. 42-24, pp. 144-164, Jet Propulsion Laboratory.

where

$$U(Z) = \frac{Z-A}{B}$$

Z = 90 - EL = zenith angle ,

EL = elevation angle ,

A, B, C, K_j^s = constants .

In the case of the optical data base, Berman found an 8th order polynomial was possible using the exponential expression instead of the 12th order required for a straight polynomial fit. After solving for the various constants, the fit below 2° elevation angle was not as close as desired and the model was modified to reduce the residual error below elevation angles of 2°. The final version used to fit the optical data base was:

$$BEND_{opt} = EXP \left\{ \sum_{j=0}^{8} \frac{K_j \, [U(Z)]^j}{1.0 + \Delta_3(Z)} \right\} - K \qquad (4)$$

where

$$\Delta_3(Z) = (Z-C_0) \, EXP \, C_1(Z-C_2)$$

and

C_0, C_1 and C_2 are empirically derived constants .

The next step is to convert the above model to fit tropospheric range error as well as refractive bending and to operate at radio frequencies instead of optical frequencies. Berman and Rockwell first modified the model expression so that changes in surface pressure and temperature could be accommodated since humidity does not affect optical refraction and is not a part of the optical correction model. Later, Berman and Rockwell further extended their modelling effort in an attempt to make the model useful for radio frequencies instead of optical frequencies.[8] The final result of this effort was a series of three modifiers to Eq. (4):

---

8. Berman, A. L., and Rockwell, S. T. (1975) A New Radio Frequency Angular Tropospheric Refraction Model, The Deep Space Network Progress Report, No. 42-25, pp. 142-149, Jet Propulsion Laboratory.

$$BEND_{rf} = F_1 F_2 F_3 BEND_{op}{}^t . \tag{5}$$

where

F_1 = f(temp) ,

F_2 = f(pressure) ,

F_3 = f(humidity) .

This seemed to be a very complicated method to make the model a function of the surface meteorological parameters and we decided to return to the basic model given in Eq. (4) and adapt it to the radar site algorithm problem. First, Eq. (4) provides a very good fit as a function of elevation angle over the entire 0° to 90° elevation angle range. Second, based upon data taken at Prospect Hill and numerous previously published papers, the refractive bending and range error at a given elevation angle are a linear function of the surface refractive index. This linear relation is good down to 2° elevation angle and acceptable down to 1°. At these very low elevation angles, the correlation between the refractive parameters and the surface refractive index is not strong using any model, due to the sensitivity of the refractive parameters to downrange tropospheric conditions. Combining the linear surface refractive index dependence and Eq. (4) yields:

$$\text{BEND or RANGE ERROR} = N_s \text{EXP} \left\{ \sum_{j=0}^{8} \frac{K_j \left[U(Z)\right]^j}{1.0 + \Delta_3(Z)} \right\} - C \tag{6}$$

where

N_s = Surface Refractive Index as defined in Eq. (1) .

The computational approach involves the calculation of the K_j's for each site. Specifically, the following equations were used in a linear stepwise regression routine which is part of the CDC 6600 statistical software:

$$BEND = N_s \cdot EXP \left\{ \sum_{j=0}^{8} K_j \left[U(Z)\right]^j \right\} - 2.47 \times 10^{-4} \text{ (deg)} \tag{7}$$

where

$$U(Z) = \frac{Z-46.625}{45.375}$$

Z = 90 - EL

EL = elevation angle (deg)

or

$$\text{RANGE ERROR} = N_s \left\{ \sum_{j=0}^{8} K_j \left[U(Z)\right]^j \right\} \text{ (meters)} \tag{8}$$

where

$$U(Z) = \frac{Z-46.625}{45.375}$$

Z = 90 - EL

EL = elevation angle (deg) .

The linear stepwise regression selected values of j which result in the selection of elements of $\left[U(Z)\right]^j{}_{j=0,8}$ which contributed to the reduction of the algorithm error in a least squares sense. The end result is that only the functions of the data which contain information about the refractive parameters are chosen to minimize the rms error. The input data for the linear stepwise regression program consist of the primary site refractivity data used in the site statistics analysis. All 27 elevation angles are used in each profile with the exception of those profiles which have ducting at certain angles. Therefore, a site with 1000 profiles provides about 27,000 samples as input to the linear stepwise regression routine. Each refractive parameter was solved for separately and a typical input would be the 27 range errors and the surface refractive index for each of 1000 profiles. The output of the regression routine consisted of each of the elements chosen out of the j= 0, 8 set and the corresponding coefficients, K_j, j = 0, 8. The elements of the range error and total refractive bending j selected were the same for all sites except Guam, however the range error element set is different from the refractive bending sets. The range error element set is j = 0, 1, 2, 3, 6, 7, and 8 while the refractive bending set is j = 0, 1, 2, 3, 4, 7, and 8. Both the total refractive bending and the elevation angle error for targets at a height of 50 km were modeled along with the range error. The modification described in Eq. (4) was added in after the linear regression and the associated constants C_0, C_1, and C_2 are the same for all sites.

A separate set of coefficients for range error, bending and angle error were calculated for each site and while the numbers are similar for all sites, there is a difference which makes each site unique. *Appendix A describes a sample refraction* parameter correction subroutine which can be used to output a true range and true elevation angle corrected for tropospheric effects when a surface refractive index, a measured range and a measured elevation angle are input. This routine is usable for any target height greater than 50 km and is explained in more detail in Appendix A.

After calculating the element set and coefficients for each site, a means of testing the algorithm and also comparing the use of various types of surface data as input was desired. Basically, each algorithm was tested against the original 2-yr data sample for each primary site. However, as a test case, at one site, the first year data sample was used to calculate the coefficients and the second year data were used to test the algorithm. The results were essentially identical to those obtained when the entire 2-yr sample was used for both coefficient calculation and algorithm testing. The basic algorithm was also tested by inputing elevation angles varying from 0.0° to 90° in 0.2° increments to verify that no discontinuities existed and that the algorithm function was monotonic.

As a comparison, the algorithm test was conducted using four different sources of the surface refractive index (N_s): the yearly mean N_s, a seasonal mean N_s, a monthly mean N_s and the individual profile N_s or real time value. The mean error and rms deviation about the mean of the error for each of 11 elevation angles was calculated for each of the four different N_s sources. Generally, the errors should decrease with the use of a more current N_s source, that is, using the seasonal mean should result in less error than using the yearly mean. The rms variability listed in the table associated with this section is the rms about the mean error since the mean error usually is a result of the imperfect fit of the model function to the elevation angle dependence rather than a result of an imperfect fit to the actual data at each elevation angle.

Table 12 lists the yearly mean N_s, the seasonal mean N_s's and the monthly mean N_s's for each site. Table 13 contains a listing of each set of coefficients used in the correction algorithm for each site. The results of the algorithm tests are presented for each site in the following sections. The elevation angle error test data are not included in this presentation since the results for the elevation angle error and the total refractive bending are essentially identical. The errors presented in the associated tables are errors only due to the imperfect fit of the correction algorithm to all of the measured data. No input N_s data errors are assumed nor are any horizontal inhomogeneity errors included.

Table 12. Surface Refractive Index Values

Site	Year	Win	Spr	Sum	Fall	Jan	Feb	Mar	Apr	May	June	July	Aug	Sept	Oct	Nov	Dec
1. Fylingdales	323	315	322	333	323	319	312	314	316	323	327	334	334	331	328	317	319
2. Thule	308	317	306	303	308	317	314	319	311	304	303	307	302	300	303	308	316
3. Clear	304	306	296	309	306	315	305	302	294	293	302	313	309	304	303	307	309
4. Eglin	342	320	350	370	333	319	317	323	344	349	359	371	372	365	347	326	325
5. Diyarbakir	288	299	288	269	299	298	299	299	297	295	275	269	268	272	298	300	300
6. Shemya	315	307	310	323	311	307	304	309	310	307	314	323	324	322	316	314	304
7. Canton Is.	375	389	375	372	368	391	389	385	379	373	371	370	373	375	366	368	369
8. Ascension Is.	358	366	369	353	351	365	369	366	376	369	362	358	350	352	349	351	355
9. Guam	378	367	375	381	379	369	366	367	369	375	379	381	381	381	380	380	376

Table 13a. Site Coefficients for Range Error Algorithm

	j	K_j	j	K_j	j	K_j	j	K_j	j	K_j	j	K_j	j	K_j
1. Fylingdales	0	-4.5560	1	0.94966	2	1.0769	3	-0.15597	6	-1.9281	7	1.5744	8	2.8196
2. Thule	0	-4.5334	1	0.94013	2	1.0329	3	-0.10986	6	-1.6453	7	1.5065	8	2.5519
3. Clear	0	-4.5268	1	0.94008	2	1.0355	3	-0.11013	6	-1.6599	7	1.5040	8	2.5610
4. Eglin	0	-4.5823	1	0.95630	2	1.1004	3	-0.18660	6	-2.0849	7	1.6253	8	2.9782
5. Diyarbakir	0	-4.4986	1	0.93767	2	1.0341	3	-0.10025	6	-1.6434	7	1.4784	8	2.5286
6. Shemya	0	-4.5442	1	0.94307	2	1.0456	3	-0.12415	6	-1.7287	7	1.5265	8	2.6306
7. Canton Is.	0	-4.6854	1	0.97548	2	1.1602	3	-0.27651	6	-2.5059	7	1.7670	8	3.4058
8. Ascension Is.	0	-4.6286	1	0.96229	2	1.1190	3	-0.21490	6	-2.2161	7	1.6711	8	3.1129
9. Guam	0	-4.6665	1	0.97234	2	1.1556	3	-0.26209	6	-2.4613	7	1.7480	8	3.3587

Table 13b. Site Coefficients for Total Refractive Bending Algorithm

	j	K_j	j	K_j	j	K_j	j	K_j	j	K_J	j	K_j	j	K_j
1. Fylingdales	0	-8.1222	1	0.44391	2	0.83186	3	-0.37243	4	-1.2639	7	1.5124	8	1.7964
2. Thule	0	-8.1128	1	0.41682	2	0.67162	3	-0.25328	4	-0.8965	7	1.3397	8	1.5081
3. Clear	0	-8.1155	1	0.42390	2	0.71672	3	-0.28422	4	-0.9987	7	1.3815	8	1.5834
4. Eglin	0	-8.1223	1	0.44751	2	0.83807	3	-0.38922	4	-1.2843	7	1.5461	8	1.8307
5. Diyarbakir	0	-8.1189	1	0.43272	2	0.77301	3	-0.32296	4	-1.1270	7	1.4307	8	1.6750
6. Shemya	0	-8.1163	1	0.42820	2	0.73828	3	-0.30367	4	-1.0404	7	1.4149	8	1.6249
7. Canton Is.	0	-8.1337	1	0.48983	2	1.0435	3	-0.57772	4	-1.7744	7	1.8399	8	2.2625
8. Ascension Is.	0	-8.1216	1	0.44860	2	0.82949	3	-0.39506	4	-1.2708	7	1.5654	8	1.8398
9. Guam	0	-8.1227	1	0.42887	2	0.82702	4	-1.2926	5	-1.1044	7	2.3455	8	1.9299

Table 13c. Site Coefficients for Elevation Angle Error Algorithm

	j	K_j	j	K_j	j	K_j	j	K_j	j	K_j	j	K_j	j	K_j
1. Fylingdales	0	-8.1478	1	0.37278	2	0.71313	4	-1.0707	5	-0.8757	7	1.9529	8	1.6299
2. Thule	0	-8.1403	1	0.36496	2	0.59532	3	-0.21876	4	-0.78219	7	1.2053	8	1.3486
3. Clear	0	-8.1437	1	0.37322	2	0.64908	3	-0.25691	4	-0.90517	7	1.2573	8	1.4405
4. Eglin	0	-8.1461	1	0.37417	2	0.70646	4	-1.0608	5	-0.88678	7	1.9821	8	1.6448
5. Diyarbakir	0	-8.1492	1	0.38315	2	0.71881	3	-0.30952	4	-1.0684	7	1.3261	8	1.5617
6. Shemya	0	-8.1440	1	0.37840	2	0.66567	3	-0.27679	4	-0.94619	7	1.2936	8	1.4857
7. Canton Is.	0	-8.1587	1	0.44922	2	0.99749	3	-0.56752	4	-1.7238	7	1.7567	8	2.1704
8. Ascension Is.	0	-8.1436	1	0.37441	2	0.68930	4	-1.0253	5	-0.87513	7	1.9856	8	1.6397
9. Guam	0	-8.1466	1	0.38431	2	0.75558	4	-1.1816	5	-1.0172	7	2.1685	8	1.7814

5.1 Fylingdales, England

Table 14 represents the expected errors when using the Fylingdales coefficients in the correction algorithm. The results follow the theoretical expectations, that is, the residual errors decrease as the input N_s data becomes more current. For example, looking at the 1° range error, the mean error is constant and the rms variability is reduced from 1.7 m using a yearly mean N_s to 1.4 m with a seasonal mean N_s, to 1.3 m with a monthly mean N_s and finally to 0.8 m with a daily or real time N_s. The peak to peak errors, although not listed, are approximately 5 or 6 times as large as the rms variabilities.

5.2 Thule, Greenland

The Thule algorithm test results are listed in Table 15. In contrast to the Fylingdales site results, the use of more current N_s data has almost no effect on the range error algorithm errors. For example, the 1° mean error of the range error algorithm is almost constant for each case and the rms variability is 1.5 m using a yearly mean N_s and 1.4 m using a daily value N_s. Again, the peak to peak errors are about 5 or 6 times as large as the rms numbers. The reasons for the poor improvement are twofold: first, the surface refractive index does not change much and second, the surface layer meteorology does not correlate well with the upper layers of the troposphere, so the surface data does not reflect the state of the entire troposphere. The refractive bending is better behaved with the 1° rms variability reduced from 0.26° using a yearly mean to 0.014° using a daily value. The above results are consistent since the refractive bending is much more sensitive to the initial gradient of the refractive index (than the range error) and the initial gradient is correlated with the surface refractive index.

5.3 Clear, Alaska

The Clear algorithm test results are listed in Table 16. The results are similar for both the range error and refractive bending at low elevation angles in that the use of monthly, seasonal and yearly mean N_s resulted in essentially the same error. The use of the profile or real time N_s, however, reduced each low angle error by one-half. At elevation angles above 5°, the range error correction does not improve with the use of more current data while the refractive bending continues to show improvement. In either case, the residual errors are small and can probably be neglected when used by the SPADATS radar systems.

5.4 Eglin AFB, Florida

Table 17 contains the Eglin algorithm test results. The Eglin surface refractive index has the greatest rms variability of any of the SPADATS sites, however the range error improvement using more current data is small even at low elevation angles. The refractive bending errors, however are reduced considerably as seen by the reduction of the 1° refractive bending error from 0.070° using a yearly mean N_s to 0.031° using a daily or real time value. One of the original assumptions made in developing the algorithm was that the range error or refractive bending is a linear function of the surface refractivity N_s. Most earlier correction algorithms were not a function of elevation angle, but consisted of several different expressions or sets of coefficients that were valid over small elevation angle ranges. In order to see if the algorithm form we selected to fit the refractive parameter data was causing the relatively poor range error performance, we applied a linear regression to each elevation angle separately. The resulting rms variabilities were not materially different from those achieved with the all elevation angle algorithm. For example, the range error rms variability at an elevation angle of 1° is 8.1 m using the all elevation angle algorithm and is reduced to 7.7 m using a linear regression on the 1° data only. The logical conclusion is that the range error correction is not a simple function of the surface refractivity, N_s, while the refractive bending is well correlated with N_s in a linear fashion.

5.5 Diyarbakir, Turkey

Table 18 contains the Diyarbakir test results using the correction algorithm. The Diyarbakir results are similar to the earlier sites with refractive bending errors improving as more current data are used while the range error improvement is small. The Diyarbakir Rawinsonde site is at an altitude of 677 m and the low average surface refractivity of 288 reflects this height. However, the algorithm coefficients are not significantly different from those at other, lower sites, therefore the Diyarbakir coefficients will be applicable for any height between sea level and 700 meters. The lower the actual site location, the higher the surface refractivity will be and the actual range errors and refractive bendings will also be larger in proportion to the surface refractivity.

5.6 Shemya, Alaska

The Shemya algorithm test results are presented in Table 19. The surface refractivity rms variability is small for this site and the algorithm test results followed the pattern set by the earlier sites with one exception. Using the monthly mean N_s resulted in worse errors than for any of the other three surface data sources. This result was true for both range error and refractive bending and was

true for all angles. The low elevation angle range error results did show an improvement when using the daily N_s values instead of the yearly mean N_s, but the higher elevation angle results were similar to the other sites with little improvement noted. The refractive bending results were very similar to the other sites in the manner in which the improvement occurred.

5.7 Canton Island

Table 20 contains the Canton Island algorithm test results. The improvement using more current data is the poorest of any of the sites studied. Even the refractive bending improvement is relatively small in comparison to the other sites where the improvement has always been good over the entire elevation angle range. The low, stable and humid marine layer that exists in the lower 150 m of atmosphere is the principle reason for the poor results using surface refractive index. The marine layer is effectively insulating the surface data from the rest of the troposphere and as a result the surface refractivity is a poor predictor of both range error and refractive bending.

5.8 Ascension Island

Table 21 contains the Ascension Island algorithm test results. Ascension Island is one of the sites with only 0000Z data and less than 500 profiles. One interesting result of this site analysis involves the range error algorithm which provided some inconsistent results in comparison with the other sites. The 1° range error results show good improvement with the use of more current data, that is, the rms variability is 1.9 m using the yearly mean N_s and 0.9 m using the daily N_s. However, at 5° and above, the rms variability of the range error fit actually gets worse when using more current data, that is, at 5°, the rms variability using the yearly mean N_s is 0.43 m and using the daily value is 0.64 meters. The refractive bending results are similar to the other sites with an improvement always occurring using more current data.

5.9 Guam

Table 22 contains the Guam algorithm test results. The Guam data set contains both 0000Z and 1200Z data and the ducting percentage is small. The algorithm results are similar to the other tropical sites, but the use of daily refractivity data was more successful than in the case of the Canton Island algorithm fit. No major differences in the results from the other sites is evident in the tabulated data.

Table 14a. Fylingdales Range Error (m) Algorithm Test Results

Elevation Angle (deg)	Daily		Monthly		Seasonal		Yearly	
	Mean	rms	Mean	rms	Mean	rms	Mean	rms
0.0	2.5	8.2	2.4	9.0	2.5	9.1	2.5	9.5
0.3	-0.5	0.7	-0.5	2.3	-0.5	2.5	-0.5	3.1
0.5	-0.2	0.6	-0.2	1.8	-0.1	2.0	-0.2	2.4
0.7	0.1	0.7	-0.1	1.6	0.1	1.7	0.1	2.1
1.0	0.3	0.7	0.3	1.3	0.3	1.4	0.3	1.7
2.0	-0.1	0.7	-0.1	0.9	-0.1	1.0	-0.1	1.1
5.0	0.2	0.5	0.2	0.5	0.2	0.5	0.2	0.5
10.0	0.5	0.3	0.5	0.3	0.5	0.3	0.5	0.3
20.0	-0.2	0.2	-0.2	0.2	-0.2	0.2	-0.2	0.2
60.0	0.00	0.06	0.00	0.06	0.00	0.06	0.00	0.06
90.0	-0.01	0.05	-0.01	0.05	-0.01	0.05	-0.01	0.05

Table 14b. Fylingdales Refractive Bending (deg) Algorithm Test Results

Elevation Angle (deg)	Daily		Monthly		Seasonal		Yearly	
	Mean	rms	Mean	rms	Mean	rms	Mean	rms
0.0	-0.011	0.165	-0.011	0.172	-0.011	0.172	-0.011	0.175
0.3	-0.029	0.036	-0.029	0.047	-0.029	0.047	-0.029	0.052
0.5	-0.013	0.024	-0.013	0.035	-0.013	0.036	-0.013	0.039
0.7	-0.003	0.017	-0.003	0.027	-0.003	0.028	-0.003	0.032
1.0	0.005	0.012	0.005	0.020	0.005	0.021	0.005	0.026
2.0	0.004	0.003	0.004	0.011	0.004	0.011	0.004	0.015
5.0	0.003	0.000	0.003	0.004	0.003	0.005	0.003	0.006
10.0	0.009	0.000	0.009	0.000	0.009	0.000	0.009	0.000
20.0	-0.004	0.000	-0.004	0.000	-0.004	0.000	-0.004	0.000
60.0	0.000	0.000	0.000	0.000	0.000	0.000	0.000	0.000
90.0	0.000	0.000	0.000	0.000	0.000	0.000	0.000	0.000

Table 15a. Thule Range Error (m) Algorithm Test Results

Elevation Angle (deg)	Daily		Monthly		Seasonal		Yearly	
	Mean	rms	Mean	rms	Mean	rms	Mean	rms
0.0	-0.9	6.5	-0.9	7.3	-0.9	7.6	-0.9	8.2
0.3	-0.5	1.2	-0.5	2.1	-0.5	2.3	-0.5	2.7
0.5	0.2	1.3	0.2	1.7	0.2	1.9	0.2	2.1
0.7	0.7	1.4	0.7	1.6	0.7	1.8	0.7	1.9
1.0	0.9	1.4	0.9	1.5	0.9	1.5	0.9	1.5
2.0	0.3	1.4	0.3	1.3	0.3	1.3	0.3	1.2
5.0	0.1	0.9	0.1	0.8	0.1	0.8	0.1	0.7
10.0	0.5	0.5	0.5	0.5	0.5	0.5	0.5	0.5
20.0	-0.1	0.3	-0.1	0.3	-0.1	0.3	-0.1	0.3
60.0	0.00	0.12	0.00	0.12	0.00	0.11	0.00	0.10
90.0	-0.01	0.11	-0.01	0.10	-0.01	0.10	-0.01	0.09

Table 15b. Thule Refractive Bending (deg) Algorithm Test Results

Elevation Angle (deg)	Daily		Monthly		Seasonal		Yearly	
	Mean	rms	Mean	rms	Mean	rms	Mean	rms
0.0	-0.061	0.160	-0.061	0.166	-0.061	0.168	-0.061	0.175
0.3	-0.029	0.044	-0.029	0.051	-0.029	0.054	-0.029	0.059
0.5	-0.006	0.029	-0.006	0.036	-0.006	0.038	-0.006	0.043
0.7	0.007	0.021	0.007	0.027	0.007	0.030	0.007	0.034
1.0	0.016	0.014	0.016	0.021	0.016	0.022	0.016	0.026
2.0	0.011	0.005	0.011	0.010	0.011	0.012	0.011	0.014
5.0	0.001	0.002	0.001	0.004	0.001	0.005	0.001	0.006
10.0	0.006	0.000	0.006	0.000	0.006	0.004	0.006	0.004
20.0	-0.002	0.000	-0.002	0.002	-0.002	0.002	0.002	0.002
60.0	0.000	0.000	0.000	0.000	0.000	0.000	0.000	0.000
90.0	0.000	0.000	0.000	0.000	0.000	0.000	0.000	0.000

Table 16a. Clear Range Error (m) Algorithm Test Results

Elevation Angle (deg)	Daily		Monthly		Seasonal		Yearly	
	Mean	rms	Mean	rms	Mean	rms	Mean	rms
0.0	0.0	7.5	0.0	9.5	0.0	9.8	0.0	10.1
0.3	-0.5	1.0	-0.5	3.9	-0.5	4.1	-0.5	4.2
0.5	0.1	1.0	0.1	3.4	0.1	3.4	0.1	3.5
0.7	0.5	1.1	0.6	3.0	0.5	3.0	0.5	3.1
1.0	0.8	1.3	0.8	2.6	0.8	2.7	0.8	2.7
2.0	0.2	1.2	0.2	1.8	0.2	1.8	0.2	1.8
5.0	0.1	0.8	0.1	0.9	0.1	0.9	0.1	0.9
10.0	0.4	0.4	0.5	0.5	0.5	0.5	0.5	0.5
20.0	-0.2	0.2	-0.2	0.3	-0.2	0.3	-0.2	0.3
60.0	0.00	0.09	0.00	0.10	0.00	0.10	0.00	0.10
90.0	-0.01	0.08	-0.01	0.09	-0.01	0.09	-0.01	0.09

Table 16b. Clear Refractive Bending (deg) Algorithm Test Results

Elevation Angle (deg)	Daily		Monthly		Seasonal		Yearly	
	Mean	rms	Mean	rms	Mean	rms	Mean	rms
0.0	-0.041	0.177	-0.041	0.188	-0.041	0.190	-0.041	0.194
0.3	-0.026	0.050	-0.026	0.067	-0.026	0.069	-0.026	0.071
0.5	-0.008	0.033	-0.007	0.050	-0.008	0.052	-0.008	0.055
0.7	0.004	0.024	0.004	0.040	0.004	0.042	0.004	0.045
1.0	0.013	0.015	0.023	0.031	0.023	0.034	0.013	0.036
2.0	0.009	0.006	0.009	0.019	0.009	0.022	0.009	0.021
5.0	0.002	0.000	0.002	0.009	0.002	0.009	0.002	0.010
10.0	0.007	0.000	0.007	0.004	0.007	0.004	0.007	0.004
20.0	-0.003	0.000	-0.003	0.000	-0.003	0.000	-0.003	0.003
60.0	0.000	0.000	0.000	0.000	0.000	0.000	0.000	0.001
90.0	0.000	0.000	0.000	0.000	0.000	0.000	0.000	0.000

Table 17a. Eglin Range Error (m) Algorithm Test Results

Elevation Angle (deg)	Daily		Monthly		Seasonal		Yearly	
	Mean	rms	Mean	rms	Mean	rms	Mean	rms
0.0	3.3	15.9	3.3	17.5	3.3	17.6	3.3	19.0
0.3	0.4	9.2	0.3	10.6	0.4	10.6	0.3	12.0
0.5	0.3	8.3	0.3	9.3	0.3	9.4	0.3	10.4
0.7	0.3	7.7	0.3	8.5	0.3	8.5	0.3	9.3
1.0	0.3	7.1	0.3	7.5	0.3	7.6	0.3	8.1
2.0	-0.2	5.5	-0.3	5.6	-0.2	5.6	0.2	5.7
5.0	0.3	3.0	0.3	3.0	0.3	3.0	0.3	3.0
10.0	0.6	1.6	0.6	1.6	0.6	1.6	0.6	1.6
20.0	-0.2	0.9	-0.2	0.9	-0.2	0.9	-0.2	0.8
60.0	0.00	0.33	0.00	0.33	0.00	0.33	0.00	0.32
90.0	-0.01	0.29	-0.01	0.28	-0.01	0.28	-0.01	0.28

Table 17b. Eglin Refractive Bending (deg) Algorithm Test Results

Elevation Angle (deg)	Daily		Monthly		Seasonal		Yearly	
	Mean	rms	Mean	rms	Mean	rms	Mean	rms
0.0	-0.030	0.246	-0.030	0.260	-0.030	0.261	-0.030	0.270
0.3	-0.015	0.090	-0.015	0.113	-0.015	0.113	-0.015	0.130
0.5	0.000	0.061	0.000	0.085	0.000	0.086	0.000	0.103
0.7	0.008	0.045	0.008	0.009	0.008	0.070	0.008	0.086
1.0	0.012	0.031	0.012	0.053	0.012	0.054	0.012	0.070
2.0	0.004	0.011	0.004	0.029	0.004	0.030	0.004	0.041
5.0	0.002	0.002	0.002	0.012	0.002	0.012	0.002	0.017
10.0	0.009	0.000	0.009	0.006	0.009	0.006	0.009	0.009
20.0	-0.004	0.000	-0.004	0.003	-0.004	0.003	-0.004	0.004
60.0	0.000	0.000	0.000	0.001	0.000	0.001	0.000	0.001
90.0	0.000	0.000	0.000	0.000	0.000	0.000	0.000	0.000

Table 18a. Diyarbakir Range Error (m) Algorithm Test Results

Elevation Angle (deg)	Daily		Monthly		Seasonal		Yearly	
	Mean	rms	Mean	rms	Mean	rms	Mean	rms
0.0	0.6	7.5	-2.3	9.4	-2.1	9.5	0.8	9.7
0.3	-0.4	2.6	-2.7	4.7	-2.5	4.8	-0.2	4.9
0.5	-0.2	2.4	-2.1	4.5	-2.0	3.9	0.1	4.0
0.7	0.1	2.5	-1.5	3.7	-1.4	3.6	0.5	3.7
1.0	0.2	2.8	-1.2	3.0	-1.1	2.9	0.6	2.9
2.0	-0.2	2.7	-1.2	2.2	-1.2	2.2	0.1	2.1
5.0	-0.1	1.7	-0.6	1.4	0.6	1.4	0.1	1.3
10.0	0.3	1.0	0.0	0.8	0.1	0.7	0.4	0.7
20.0	0.2	0.6	0.4	0.5	0.4	0.5	0.2	0.4
60.0	0.0	0.2	-0.1	0.2	-0.1	0.2	0.0	0.2
90.0	0.0	0.2	-0.1	0.2	-0.1	0.2	0.0	0.1

Table 18b. Diyarbakir Refractive Bending (deg) Algorithm Test Results

Elevation Angle (deg)	Daily		Monthly		Seasonal		Yearly	
	Mean	rms	Mean	rms	Mean	rms	Mean	rms
0.0	-0.009	0.193	-0.031	0.206	-0.029	0.207	-0.007	0.209
0.3	-0.003	0.084	-0.021	0.104	-0.019	0.106	-0.002	0.107
0.5	0.004	0.059	-0.010	0.080	-0.009	0.082	0.006	0.084
0.7	0.013	0.062	0.002	0.084	0.003	0.085	0.017	0.085
1.0	0.014	0.032	0.004	0.055	0.005	0.056	0.017	0.057
2.0	0.008	0.010	0.000	0.028	0.001	0.029	0.004	0.031
5.0	0.003	0.001	-0.001	0.011	-0.002	0.012	0.004	0.012
10.0	0.007	0.000	0.005	0.006	0.005	0.006	0.007	0.006
20.0	-0.003	0.000	-0.004	0.003	-0.004	0.003	-0.003	0.003
60.0	0.000	0.000	0.000	0.001	0.000	0.001	0.000	0.000
90.0	0.000	0.000	0.000	0.000	0.000	0.000	0.000	0.000

Table 19a. Shemya Range Error (m) Algorithm Test Results

Elevation Angle (deg)	Daily		Monthly		Seasonal		Yearly	
	Mean	rms	Mean	rms	Mean	rms	Mean	rms
0.0	-0.2	6.4	1.9	7.7	0.7	7.4	-0.2	7.5
0.3	-0.2	0.7	1.6	3.0	0.6	2.6	-0.2	2.8
0.5	0.4	0.5	2.0	2.4	1.1	2.0	0.4	2.2
0.7	0.7	0.6	2.2	2.2	1.3	1.7	0.7	1.8
1.0	0.8	0.7	2.1	1.8	1.4	1.4	0.8	1.5
2.0	0.2	0.7	1.1	1.2	0.6	1.0	0.2	1.0
5.0	0.2	0.4	0.7	0.6	0.4	0.5	0.2	0.5
10.0	0.5	0.2	0.7	0.3	0.6	0.3	0.5	0.3
20.0	-0.2	0.1	0.0	0.2	-0.1	0.1	-0.2	0.1
60.0	0.00	0.06	0.06	0.07	0.03	0.05	0.00	0.05
90.0	0.01	0.04	0.04	0.06	0.01	0.05	0.00	0.05

Table 19b. Shemya Refractive Bending (deg) Algorithm Test Results

Elevation Angle (deg)	Daily		Monthly		Seasonal		Yearly	
	Mean	rms	Mean	rms	Mean	rms	Mean	rms
0.0	-0.061	0.141	-0.044	0.150	-0.054	0.148	-0.061	0.150
0.3	-0.026	0.041	-0.012	0.056	-0.020	0.054	-0.026	0.056
0.5	-0.006	0.028	0.006	0.042	0.000	0.041	-0.006	0.042
0.7	0.006	0.022	0.017	0.033	0.010	0.032	0.006	0.035
1.0	0.013	0.014	0.023	0.026	0.018	0.024	0.014	0.026
2.0	0.008	0.005	0.015	0.014	0.011	0.012	0.008	0.014
5.0	0.001	0.001	0.005	0.006	0.003	0.005	0.001	0.006
10.0	0.007	0.000	0.009	0.003	0.008	0.002	0.007	0.002
20.0	-0.003	0.000	-0.002	0.002	-0.002	0.001	0.003	0.001
60.0	0.000	0.000	0.000	0.000	0.000	0.000	0.000	0.000
90.0	0.000	0.000	0.000	0.000	0.000	0.000	0.000	0.000

Table 20a. Canton Island Range Error (m) Algorithm Test Results

Elevation Angle (deg)	Daily		Monthly		Seasonal		Yearly	
	Mean	rms	Mean	rms	Mean	rms	Mean	rms
0.0								
0.3								
0.5								
0.7	1.5	1.0	2.1	2.3	2.2	2.3	1.5	2.8
1.0	-0.1	1.0	0.4	1.8	0.4	1.8	-0.1	1.9
2.0	-1.1	1.1	-0.7	1.3	-0.7	1.3	-1.1	1.2
5.0	0.3	0.6	0.5	0.6	0.5	0.6	0.3	0.6
10.0	0.7	0.3	0.8	0.3	0.8	0.3	0.7	0.3
20.0	-0.2	0.2	-0.2	0.2	-0.2	0.2	-0.2	0.2
60.0	0.00	0.08	0.02	0.08	0.02	0.08	0.00	0.06
90.0	-0.01	0.06	0.00	0.06	0.00	0.06	-0.01	0.05

Table 20b. Canton Island Refractive Bending (deg) Algorithm Test Results

Elevation Angle (deg)	Daily		Monthly		Seasonal		Yearly	
	Mean	rms	Mean	rms	Mean	rms	Mean	rms
0.0								
0.3								
0.5								
0.7	0.036	0.074	0.041	0.078	0.042	0.078	0.036	0.086
1.0	0.007	0.033	0.012	0.040	0.012	0.040	0.007	0.046
2.0	-0.015	0.006	-0.011	0.015	-0.011	0.015	-0.014	0.018
5.0	0.002	0.000	0.004	0.005	0.004	0.005	0.002	0.007
10.0	0.014	0.000	0.015	0.002	0.015	0.002	0.014	0.002
20.0	-0.005	0.000	-0.005	0.001	-0.005	0.001	-0.005	0.001
60.0	0.000	0.000	0.000	0.000	0.000	0.000	0.000	0.000
90.0	0.000	0.000	0.000	0.000	0.000	0.000	0.000	0.000

NOTE: High incidence of ducting below 0.7° precluded meaningful test results.

Table 21a. Ascension Island Range Error (m) Algorithm Test Results

Elevation Angle (deg)	Daily		Monthly		Seasonal		Yearly	
	Mean	rms	Mean	rms	Mean	rms	Mean	rms
0.0	2.3	7.7	2.4	9.5	3.2	9.5	2.2	10.2
0.3	0.6	1.3	0.6	3.8	1.3	3.9	0.5	4.4
0.5	0.6	0.5	0.6	2.8	1.2	2.9	-0.5	3.2
0.7	0.5	0.7	0.6	2.2	1.1	2.3	0.4	2.5
1.0	0.3	0.9	0.4	1.7	0.8	1.9	0.2	1.9
2.0	-0.4	1.1	-0.3	1.1	0.0	1.2	-0.4	1.1
5.0	0.3	0.6	0.3	0.5	0.5	0.6	0.3	0.4
10.0	0.6	0.4	0.6	0.3	0.7	0.3	0.6	0.2
20.0	-0.2	0.2	-0.2	0.2	-0.1	0.2	-0.2	0.1
60.0	0.00	0.08	0.00	0.05	0.02	0.06	0.00	0.04
90.0	-0.01	0.06	-0.01	0.05	0.00	0.05	-0.01	0.04

Table 21b. Ascension Island Refractive Bending (deg) Algorithm Test Results

Elevation Angle (deg)	Daily		Monthly		Seasonal		Yearly	
	Mean	rms	Mean	rms	Mean	rms	Mean	rms
0.0	-0.073	0.163	-0.072	0.177	-0.065	0.177	-0.074	0.183
0.3	-0.024	0.062	-0.023	0.078	-0.018	0.078	-0.025	0.083
0.5	0.000	0.041	0.001	0.057	0.006	0.057	0.000	0.062
0.7	0.012	0.029	0.013	0.044	0.017	0.045	0.012	0.049
1.0	0.017	0.018	0.018	0.032	0.021	0.032	0.017	0.036
2.0	0.005	0.006	0.005	0.017	0.008	0.017	0.004	0.020
5.0	0.002	0.002	0.002	0.007	0.003	0.007	0.001	0.008
10.0	0.010	0.000	0.010	0.004	0.010	0.004	0.010	0.004
20.0	-0.004	0.000	-0.004	0.002	-0.004	0.002	-0.004	0.002
60.0	0.000	0.000	0.000	0.000	0.000	0.000	0.000	0.000
90.0	0.000	0.000	0.000	0.000	0.000	0.000	0.000	0.000

Table 22a. Guam Range Error (m) Algorithm Test Results

Elevation Angle (deg)	Daily		Monthly		Seasonal		Yearly	
	Mean	rms	Mean	rms	Mean	rms	Mean	rms
0.0	4.7	10.1	5.1	10.9	4.8	10.8	5.7	11.0
0.3	1.9	2.5	2.3	3.6	2.0	3.7	2.6	3.8
0.5	1.0	1.0	1.2	2.4	1.0	2.4	1.6	2.8
0.7	0.4	0.9	0.7	2.0	0.5	2.0	1.0	2.3
1.0	-0.1	0.9	0.2	1.8	-0.1	1.8	-0.4	2.0
2.0	-0.8	0.9	-0.6	1.2	-0.7	1.3	-0.4	1.4
5.0	0.3	0.5	0.4	0.6	0.3	0.6	0.5	0.7
10.0	0.7	0.3	0.7	0.3	0.7	0.3	-0.8	0.4
20.0	-0.2	0.2	-0.2	0.2	-0.2	0.2	-0.2	0.2
60.0	0.0	0.1	0.0	0.1	0.0	0.1	0.0	0.1
90.0	0.0	0.1	0.0	0.1	0.0	0.1	0.0	0.1

Table 22b. Guam Refractive Bending (deg) Algorithm Test Results

Elevation Angle (deg)	Daily		Monthly		Seasonal		Yearly	
	Mean	rms	Mean	rms	Mean	rms	Mean	rms
0.0	-0.079	0.183	-0.075	0.188	-0.078	0.188	-0.070	0.188
0.3	-0.008	0.074	-0.006	0.080	-0.008	0.081	-0.002	0.081
0.5	0.006	0.045	0.008	0.051	0.006	0.052	0.011	0.052
0.7	0.012	0.030	0.015	0.037	0.013	0.037	0.017	0.037
1.0	0.014	0.018	0.016	0.025	0.014	0.025	0.018	0.025
2.0	0.002	0.006	0.003	0.012	0.002	0.012	0.005	0.012
5.0	0.004	0.000	0.005	0.005	0.005	0.005	0.005	0.005
10.0	0.011	0.000	0.012	0.003	0.012	0.003	0.012	0.003
20.0	-0.005	0.000	-0.005	0.000	-0.005	0.000	-0.005	0.001
60.0	0.001	0.000	0.002	0.000	0.001	0.000	0.001	0.000
90.0	0.000	0.000	0.000	0.000	0.000	0.000	0.000	0.000

6. SUMMARY AND CONCLUSIONS

An analysis of the tropospheric refractive environment surrounding the U.S. Air Force SPADATS radar sites has been presented with the limitations of the Rawinsonde data base that made available by USAFETAC. Individual site statistics describing the behavior of range error and refractive bending at each location have been presented in tabular form allowing for ready comparison of the various climatological regions in which the sites are located.

Generally, unless highly precise radars are used which operate at very low elevation angles and require highly accurate tropospheric corrections, the refractive effects at the various sites are so similar as to be almost indistinguishable. The original intent in providing a correction algorithm using different types of surface refractivity, either averages or real time values, was to offer a choice between the various surface refractivity data sources. The final result generally showed little improvement over the use of the yearly mean N_s unless the real time daily value was used. The final algorithm was designed as a general purpose correction algorithm and provides a reasonable fit to the elevation angle dependence of the refractive parameters and also provides an acceptable fit to the day to day variations of these parameters. Lower refractive parameter residuals are possible if additional complexity can be tolerated or a restricted elevation angle range is acceptable. The attempt to calculate the effects of horizontal inhomogeneity was only partially successful due to the generally wide spacing of the secondary sites, but upper limits on errors due to horizontal variations in the troposphere were calculated.

7. RECOMMENDATIONS

After analyzing the mass of refractive data that were available and reducing the data to a set of statistics for each site, the numbers became more manageable and some recommendations can be made based upon a few assumptions. The SPADATS radars located at the nine sites analyzed operate at 425 MHz, 1300 MHz, and 5400 MHz. The radars operating at 425 MHz, with the exception of the AN/FPS-85 at Eglin AFB, have severe ionospheric refraction correction problems. The data presented by Klobuchar and Allen[1] provides an indication of the maximum ionospheric range errors that could be expected during conditions of solar sunspot maximum periods. At 425 MHz, the ionospheric range errors vary from a minimum of about 30 m to a maximum of 1000 m at low elevation angles. Current techniques allow prediction of these ionospheric errors to within 10 percent or from 3 to 100 meters. Projected ionospheric correction techniques may reduce these

errors by a factor of four (Allen[9]). The typical ionospheric correction precision seems to be of the order of 10 m with a corresponding precision in angle error. The Eglin radar is an exception due to the use of real time ionospheric data to provide an update capability. Since the typical tropospheric range error at 5° elevation angle is about 25 m, it is obvious that the ionospheric effects far outweigh the tropospheric effects at 425 MHz. Therefore, for the sites operating at 425 MHz, except Eglin, a simple yearly mean range and angle error correction which is only a function of elevation angle will suffice. This corresponds to the use of a yearly mean surface index of refraction in the correction algorithms presented in this report. The AN/FPS-85 radar should use at a minimum a real time surface index of refraction to provide a tropospheric correction commensurate with the radar precision and accuracy.

The ionospheric range errors at 1300 MHz are almost an order of magnitude smaller than at 425 MHz. Typical range errors due to the ionosphere range from 5 to 100 m with a corresponding correction accuracy from 0.5 to 10 meters. The ionospheric and tropospheric effects are comparable in this case and the real time surface index of refraction should be used for the correction of the tropospheric effects.

One SPADATS radar operates in the C-Band frequency range where the effects of the ionosphere are very small and the tropospheric refraction effects are larger than the ionospheric errors. The surface index of refraction measured on a real time basis should be used at this site also.

The use of the surface index of refraction provides a good predictor of the tropospheric effects when considered over a long period of time and when the errors are calculated and presented in a rms form. It should be noted, however, that during certain periods of time, particularly under ducting conditions, the predicted tropospheric effects and the actual effects will differ by an amount greater than the standard deviation data presented earlier would indicate. The only hope of reducing these types of errors is the use of real time Rawinsonde data which is usually impractical in an operational situation.

---

9. Allen, R.S. (1977) Considerations Relative to Adapting TRANSIT Observations to Predicting Radar Range Correction, AFGL-TR-77-0004, AD AO38238.

References

1. Klobuchar, J.A., and Allen, R.S. (1976) Maximum Ionospheric Range Error For Air Defense Command Radars, AFGL-TR-76-0042, AD BO11322L.
2. Gallop, M.A., and Telford, L.E. (1975) Use of atmospheric emission to estimate refractive errors in a non-horizontally stratified troposphere, Radio Sci. 10(No. 11):935-945.
3. Zanter, D.L. et al (1976) The Effect of Atmospheric Refraction on the Accuracy of Laser Ranging Systems, NASA-CR-146313.
4. Vicker, W.W., and Lopez, M.E. (1975) Low angle radar tracking errors induced by nonstratified atmospheric anomalies, Radio Sci. 10(No. 5):491-505.
5. Bean, B.R., and Thayer, G.D. (1959) CRPL Exponential Reference Atmosphere, Nat. Bur. Stand. Monograph No. 4.
6. Bean, B.R., and Dutton, E.J. (1966) Radio Meteorology, Nat. Bur. Stand. Monograph No. 92.
7. Berman, A.L., and Rockwell, S.T. (1974) A New Angular Tropospheric Refraction Model, The Deep Space Network Progress Report, No. 42-24, pp. 144-164, Jet Propulsion Laboratory.
8. Berman, A.L., and Rockwell, S.T. (1975) A New Radio Frequency Angular Tropospheric Refraction Model, The Deep Space Network Progress Report, No. 42-25, pp 142-149, Jet Propulsion Laboratory.
9. Allen, R.S. (1977) Considerations Relative to Adapting TRANSIT Observations to Predicting Radar Range Correction, AFGL-TR-77-0004, AD AO38238.

Appendix A

Correction Algorithm Form

The basic tropospheric refraction correction algorithm provides the range error, refractive bending and elevation angle error for a target height of 50 km and for elevation angles from 0.0 to 90.0°. Most space tracking systems will involve targets higher than 50 km and a means of converting the algorithm output to corrections useful for these targets is needed. The 50 km height was chosen to represent an altitude which divides the troposphere and the ionosphere. This routine utilizes the simple geometry of the ray path to find the true range and elevation angle. This geometry is illustrated in Figure A1. The inputs to the correction routine are: (1) surface refractivity, (2) measured radar range, (3) measured radar elevation angle, and (4) ionospheric range error if applicable. The outputs are true range to target and true elevation angle. A sample correction routine as used for algorithm verification during this study is presented below.

```
      SUBROUTINE REFRAC (ANS, EL, RGM, DRION, RGTR, ELTR)
C     ANS = SURFACE REFRACTIVITY IN N-UNITS
C     EL  = MEASURED RADAR ELEVATION ANGLE IN DEGREES
C     RGM= MEASURED RADAR RANGE IN KM
C     DRION = IONOSPHERIC RANGE ERROR TO TARGET IN KM
C     RGTR = TRUE RANGE TO TARGET IN KM
C     ELTR = TRUE ELEVATION ANGLE TO TARGET IN DEGREES
      DIMENSION R(10), B(10), E(10), NR(10), NB(10), NE(10)
      DATA R/    /, DATA NR/    /, DATA B/    /, DATA NB/    /
      DATA E/    /, DATA NE/    /
C     PROPER CONSTANTS FOR STATION WHERE CORRECTIONS ARE DESIRED
      SHOULD BE ENTERED IN DATA STATEMENTS.
      A=6370.
```

```
C     A IS RADIUS OF EARTH IN KM
      A50=A+50.
C     THE NEXT SECTION OF THE PROGRAM CALCULATES THE TROPOSPHERIC
C     REFRACTION PARAMETERS FOR A TARGET HEIGHT OF 50 KM. NOTE THAT
C     THIS ROUTINE ASSUMES THE ACTUAL TARGET TO BE ABOVE 50 KM.
      U=(43.375-EL)/45.375
      X=0.
      DO 1 I=1,7
    1 X=X+R(I)*(U**NR(I))
      DEL=1.-(EL-0.55)*EXP(-1.08*(EL+1.85))
      X=X/DEL
      RER=ANS*EXP(X)
C     RER = RANGE ERROR IN METERS
      X=0.
      DO 3 I=1,7
    3 X=X+B(I)*(U**NB(I))
      DEL=1.-(EL-0.6)*EXP(-0.985*(EL+3.07))
      X=X/DEL
      BER=ANS*(EXP(X)-2.47E-04)
C     BER = REFRACTIVE BENDING IN DEGREES
      X=0.
      DO 5 I=1,7
    5 X=X+E(I)*(U**NE(I))
      X=X/DEL
      EER=ANS*(EXP(X)-2.47E-04)
C     EER = ELEVATION ANGLE ERROR
C     THE NEXT FEW STATEMENTS CONVERT DEGREES TO RADIANS AND M TO KM
      ELR=EL*0.017453
      EERR=EER*0.017453
      BERR=BER*0.017453
      REK=RER*1000.
C     THE NEXT SECTION CONVERTS THE "50 KM" CORRECTIONS TO THE
C     ACTUAL TARGET HEIGHT.
      APR=A5-*SQRT(1.-(((A/A50)*COS(ELR-EERR))**2))-A*SIN(ELR-EERR)
C     APR = TROPOSPHERIC RANGE TO AN ALTITUDE OF 50 KM FOR THE
C     GIVEN RADAR ELEVATION ANGLE
      RGTR=SQRT(APR*APR+(RGM-APR-REK-DRION)**2)+2.*APR*(RGM-APR-
     1  REK-DRION)
     2*COS(BERR-EERR)
      ELTR=EL-EER-57.29578*ASIN((RGM-APR-REK-DRION)/RGTR)*SIN(BERR-
     1  EERR))
      RETURN
      END
```

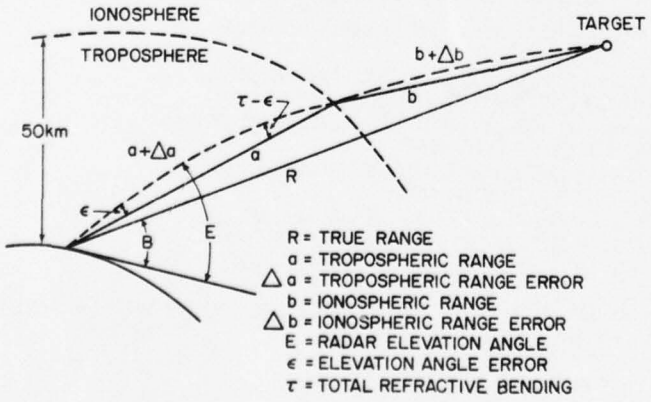


Figure A1. Schematic Representation of Ray Path